AD_____

Award Number: W81XWH-10-1-0963

TITLE: Characterization of RACK7 as a Novel Factor Involved in BRCA1 Mutation Mediated Breast Cancer

PRINCIPAL INVESTIGATOR: Inder M. Verma, Ph.D.

CONTRACTING ORGANIZATION: Salk Institute for Biological Studies
La Jolla, CA 92037

REPORT DATE: October 2012

TYPE OF REPORT: Final

PREPARED FOR: U.S. Army Medical Research and Materiel Command
Fort Detrick, Maryland 21702-5012

REPORT DOCUMENTATION PAGE

Form Approved
OMB No. 0704-0188

1. REPORT DATE *(DD-MM-YYYY)*	2. REPORT TYPE	3. DATES COVERED *(From - To)*
October 2012	Final	15 September 2010 - 14 September 2012

4. TITLE AND SUBTITLE
Characterization of RACK7 as a Novel Factor Involved in BRCA1 Mutation Mediated Breast Cancer

5a. CONTRACT NUMBER

5b. GRANT NUMBER
W81XWH-10-1-0963

5c. PROGRAM ELEMENT NUMBER

6. AUTHOR(S)
Inder Verma, Quan Zhu, Martin Preyer, and Amy Rommel

E-Mail: verma@salk.edu, qzhu@salk.edu, mpreyer@salk.edu, arommel@salk.edu

5d. PROJECT NUMBER

5e. TASK NUMBER

5f. WORK UNIT NUMBER

7. PERFORMING ORGANIZATION NAME(S) AND ADDRESS(ES)
Salk Institute for Biological Studies
La Jolla, CA 92037

8. PERFORMING ORGANIZATION REPORT NUMBER

9. SPONSORING / MONITORING AGENCY NAME(S) AND ADDRESS(ES)
U.S. Army Medical Research and Materiel Command
Fort Detrick, Maryland 21702-5012

10. SPONSOR/MONITOR'S ACRONYM(S)

11. SPONSOR/MONITOR'S REPORT NUMBER(S)

12. DISTRIBUTION / AVAILABILITY STATEMENT
Approved for Public Release; Distribution Unlimited

13. SUPPLEMENTARY NOTES

14. ABSTRACT

Though BRCA1 has been shown to play a role in DNA end resection, likely critical in the cell's decision to undergo homologous recombination or non-homologous end joining repair pathways, much of BRCA1 function remains unknown. To identify genes that cooperate with BRCA1 in DNA damage response and tumor suppression, we performed a lentiviral vector based cDNA library screen. ZMYND8 (zinc finger Mynd-type containing 8), previously Rack7 (receptor for activated C kinase) or Prkcbp1 (protein kinase C binding protein 1), was identified in our screen as a candidate gene that could modulate the DNA damage hypersensitivity in cells lacking BRCA1. Biochemical data indicates that ZMYND8 might be involved in chromatin reorganization surrounding a stalled fork, which may be vital in preventing collapse and granting genomic stability. Overexpression of ZMYND8 in breast, ovarian, and several other malignancies, could be a novel mechanism to overcome replica-tion stress resulting from BRCA1 dysfunction. This suggests that ZMYND8 and BRCA1 could function epistatically, a phenomenon we continue to investigate using our lab-generated mouse models. In conclusion, our novel findings demonstrate that ZMYND8 is required to prevent the reversal of stalled replication forks, and thereby contributes to the preservation genomic stability under replication stress.

15. SUBJECT TERMS
15. SUBJECT TERMS ZMYND8, RACK7, Prkcbp1, BRCA1, Genomic Stability, Replication Fork, DNA Damage Response, DNA double strand break, ATM, phosphorylation, transgenic mouse model

16. SECURITY CLASSIFICATION OF:			17. LIMITATION OF ABSTRACT	18. NUMBER OF PAGES	19a. NAME OF RESPONSIBLE PERSON
a. REPORT	b. ABSTRACT	c. THIS PAGE			USAMRMC
U	U	U	UU	72	19b. TELEPHONE NUMBER *(include area code)*

Table of Contents

Page

INTRODUCTION

The BRCA1 and BRCA2 tumor suppressors play important roles in the repair of damaged DNA [1, 2], and cells lacking either of these proteins are hypersensitive to a variety of DNA damaging agents [3-7]. The function of BRCA2 has been linked to the recruitment and loading of the recombination protein RAD51 onto single-stranded overhangs created at a double strand break [8]. The function of BRCA1 is less well-defined, but it has been shown to play a role in DNA end resection at the break [9, 10] and is therefore critical in the decision-making between homologous recombination and non-homologous end joining repair pathways [11, 12]. To identify genes that cooperate with BRCA1 in the DNA damage response and tumor suppression, we have performed a screen using a lenti-viral vector based cDNA library which expresses 17,500 full length human and mouse genes. The gene ZMYND8 (zinc finger Myndtype containing 8), which was previously called Rack7 (receptor for activated C kinase) or Prkcbp1 (protein kinase C binding protein 1), was indentified in our screen as a candidate gene that could modulate the DNA damage hypersensitivity of cells lacking BRCA1. Nothing is known about the biological function of ZMYND8; however, a very recent proteomics study has demonstrated its association with several chromatin modifying enzymes and suggested that ZMYND8 might be involved in the regulation of transcription [13]. Interestingly, the locus encoding *zmynd8* gene was recently identified by the cancer genome atlas research network as being amplified in ovarian cancer[14].

BODY

Task 1. Characterization of the biochemical functions of ZMYND8.
As reported previously in our *Annual Report 2011*, we have identified and characterized ZMYND8 as a novel substrate of ATR and ATM kinases. ZMYND8 is phosphorylated at serine 1060 after DNA double strand breaks and replication stress. Cells lacking ZMYND8 are hypersensitive to agents that induce replication stress, but have normal survival after ionizing radiation. We have further characterized the biochemical function of ZMYND8, which is required for stabilizing stalled replication forks and to prevent fork reversal after nucleotide depletion with hydroxyurea. We have recently submitted a manuscript reporting these findings for publication in Nature (Preyer M and Verma IM, "ZMYND8 protects cancer cells against replication stress through stabilization of stalled forks", Nature, *submitted*). The manuscript including all figures is attached in the Appendix and sub-task summaries are below for the now completed Task 1 (except for successful purification of fragment in Task 1d).

Task 1.a. Time course and dose response studies of ZMYND8 (Rack7) phosphorylation after IR
Our preliminary data had indicated that ectopically expressed ZMYND8 is modified by phosphorylation in cells that were exposed to ionizing radiation (IR). We were able to detect the phosphorylation of endogenous ZMYND8 after the induction of DNA double strand breaks with IR using an antibody that was raised against phospho-serine in the context of an ATM target site (serine-glutamine, SQ) [15]. Detailed time course studies revealed that the phosphorylation of ZMYND8 occurred with interestingly slow kinetics compared toother known ATM substrates and only at high doses of ionizing radiation above 4 Gy. Phospho-ZMYND8 stayed below the detection limit until 30 minutes and reached a plateau only at 60 minutes after the induction of double strand breaks with high doses of IR. Thus, ZMYND8 is a novel protein that is phosphorylated in response to high-dose IR with slow kinetics.

Task 1.b. Phosphorylation of ZMYND8 (Rack7) in response to other sorts of DNA damage
We tested the effect of different DNA damaging agents and found that ZMYND8 was weakly phosphorylated when cells were treated with the radiomimetic drug adriamycin (ADR, also known as doxorubicin). The topoisomerase poison etoposide (VP-16) induced a very robust and high level of ZMYND8 phosphorylation. Because topoisomerases are most active in S-phase to relieve the tensile stress associated with moving replication forks, we tested whether ZMYND8 was also phosphorylated in response to other forms of replication stress. Indeed, the treatment with hydroxyurea (HU), which stalls replication forks through the depletion of deoxynucleosides, also caused a strong phosphorylation of ZMYND8. However, unlike ionizing radiation, which caused a very slow increase in phospho-ZMYND8, the treatment with HU resulted in more rapid phosphorylation of ZMYND8, which occurred in cells with similar kinetics. Thus, we have found that ZMYND8 Ser1060 is phosphorylated after several genotoxic agents including HU-induced replication stress.

Task 1.c. The requirement for ATM in the IR-induced ZMYND8 (Rack7) phosphorylation will be tested using an ATM inhibitor (KU55933) and ATM deficient-cells (A-T fibroblasts)
A competitive inhibitor of ATM serine/threonine kinase activity (KU55933) abolished the IR-induced

phosphorylation of ZMYND8, demonstrating that ATM kinase is required for ZMYND8 phosphorylation. When we mutated the serine 1060 of ZMYND8 to alanine (S1060A), the phosphorylation of the protein was no longer detected following IR. This serine is in the context of an ATM/ATR consensus site (SQ-site) which further supports the notion that the ZMYND8 phosphorylation is ATM dependent.

Task 1.d. The in vitro phosphorylation of ZMYND8 (RACK7) peptide by ATM
Thus far, we have not been able to successfully purify a ZMYND8 fragment encompassing the phosphorylation site from bacteria for the use in immune-complex kinase assays, in order to show that ATM is able to phosphorylate ZMYND8 directly. The difficulty to purify the fragment may be due to the fact that the phosphorylation site S1060 is immediately adjacent to the myndtype zinc finger, which makes this construct possibly difficult to purify due to folding, but efforts to optimize the purification are ongoing.

Task 1.e. Mechanistic study of the putative association of ZMYND8 (Rack7) with cell death after DNA damage
We first tested whether the ZMYND8 protein is required for survival of cells in response to DNA double strand breaks induced by IR. Knock-down of ZMYND8 by siRNA did not alter the survival of Hela or U2OS cells after different doses of IR. In contrast, knock-down of the BRCA1 protein resulted in decreased survival of cells due to the well-known defect in DNA repair in BRCA1-deficient cells [1, 2]. Thus, our present data clearly does not support a major role for ZMYND8 in cell death after IR.

Because we found that ZMYND8 was rapidly and strongly phosphorylated when DNA replication was stalled with HU, we tested whether ZMYND8 was required for survival after replication stress induced by HU. We used lentiviral vectors to deliver different shRNAs into U2OS cells to knock down the expression of ZMYND8. We then tested the sensitivity of these cells, which lack ZMYND8, to different doses of HU in a clonogenic survival assay. Cells lacking ZMYND8 protein were significantly more sensitive to HU than the control cells expressing an shRNA against luciferase. Thus, ZMYND8, which is rapidly phosphorylated after replication stress, is also required for the recovery of cells from this stress. Cells lacking the BRCA1 protein showed a similar sensitivity to replication stress by HU as ZMYND8-knockdown cells. Interestingly, the simultaneous knockdown of both, ZMYND8 and BRCA1, did not further increase the sensitivity to HU. This mutual epistasis could indicate that ZMYND8 and BRCA1 act in the same pathway in the recovery from HU-induced replication fork stalling.

To investigate the effect of ZMYND8 knockdown on stalled replication forks more directly, we performed a DNA fiber assay. In this assay, the track of replication forks in cells is directly labeled through the incorporation of iodo-deoxyuridine or, after HU-induced stalling, chlorodeoxyuridine. Thus, the stalling of replication forks as well as the restart after removal of HU can be directly imaged with fluorescently labelled antibodies against the halogenated nucleotides. Using this technique, we found that the ZMYND8 knockdown cells and control cells showed similar replication tracks in the absence of replication stress. However, we found that shZMYND8 cells exhibit a defect in the restart of replication forks after only one hour of HU treatment. Therefore we conclude that ZMYND8 is required for the recovery from replication stress and thus for the survival after HU. In the absence of ZMYND8 protein, cells fail to restart stalled forks promptly and are hypersensitive to agents that cause replication stress. We are currently testing whether BRCA1 function in the same pathway after replication stress.

Task 2. Analyze the expression levels of RACK7 in human and mouse mammary tumors. We have performed an extensive *in silico* analysis of ZMYND8 expression using a consistently normalized set of gene expression data[17] containing several thousand expression profiles from the Gene Expression Atlas. This analysis demonstrated that ZMYND8 is highly overexpressed in ovarian cancer and breast cancer. Furthermore, we found that ZMYND8 is also highly expressed in several other cancers. The results of this analysis of ZMYND8 expression are shown in Figure 1.

Task 2.a. Obtain and analyze RNA samples from 5 more human BRCA1 mutant tumors.
We continue to collect more human BRCA1-mutant tumors from Dr. Petra Nederlof at the Netherland Cancer Institute. While waiting for the access, as previously reported in our Annual Report 2011, we analyzed 9 breast tumors with no known BRCA1-mutations and performed real time RT-PCR experiments to quantify the levels of RACK7 mRNA as shown in Figure 2. We found 4 samples that have over-expression of RACK7 which is associated with higher grade of breast cancer staging (T2 vs T1).

Task 2.b. Analyze expression levels of RACK7 in mouse mammary glands and tumors.
We harvested tissues from wild-type mammary glands and BRCA1-deficient breast tumors. RNA was

prepared and real time RT-PCR was performed to measure the levels of RACK7 mRNA in these samples as shown in Figure 3. There was over 300 fold induction of RACK7 expression in a mammary tumor than the control normal mammary glands. We continue to collect and analyze more age matched mouse tumor samples.

Task 3. Characterization of biological functions of RACK7 in vivo.

Task 3a. Generation of transgenic animals using lentiviral vectors expressing tagged RACK7 under CAG promoter or mammary gland specific promoter (months 2-4 remaining)
We have generated an HA-tagged RACK7 lentiviral expression vectors. As shown in figure 4, the protein is being expressed in cultured cell lines. The construct has been submitted to the Salk Transgenic Facility for the generation of transgenic mice. Genotyping is currently being carried out using lentiviral specific primers and human RACK7 specific primers by detection of HA tag for germline transmission.

Task 3b. Design and validate shRNA against mouse RACK7
The mouse RACK7 shRNA had been originally designed based on the human RACK7 shRNA sequence which should have efficiently depleted the protein. The sequence and genomic location of the original shRNA is shown in Figure 5. Upon transfection however, this shRNA proved to be inefficient, yielding little to no knockdown of ZMYND8/RACK7 as shown in Figure 6. A new shRNA was ordered with the sequence CGCCACCTTTAGAATTTCCAA for the mature sense strand. Western blot analysis show efficient knockdown of ~ 50% by 48 hours after transfection of MEFs shown in Figure 7.

Task 3c. Generation of transgenic animals using lentiviral vectors expressing shRNA against mouse RACK7 (months 3-8) We have validated the shRNA as proposed. However, it has been reported that the deletion of mouse RACK7 is embryonically lethal (http://www.sanger.ac.uk/mouseportal/phenotyping/mbdz/viability-at-weaning/). Therefore, we have modified the protocol by designing an inducible shRNA with tissue-specific promoter to knockdown the mouse RACK7. For this we have cloned the shRNA into pBOB-CAG LoxP MCS expression vector. Virus is being generated and will be sent to the Salk transgenic facility once purified and ready for transgenic mouse generation.

Task 3d-g. Breeding of floxed BRCA1 with floxed p53 mice and K14-CRE mice (months 7-12)
We had floxed BRCA1 MM-TV-CRE and floxed p53 mice mating pairs in hand. However, the mating yielded no pups, likely a result of the age of the floxed p53 mice upon receipt from a collaborating laboratory. Due to the lack of transgenic mice from this cross, we ordered a suitable transgenic mouse from JAX. This mouse STOCK *Trp531*^{tm1Brd} *Brca1*^{tm1Aash}Tg(LGBcre)74Acl/J should work as a suitable mating pair for crossing to our transgenic shZMYND8 mouse now being generated. We expect this process will take 6 months to obtain a population of mice to use for time trials for tumor formation and phenotype analysis and 18 months to full completion of tasks proposed in this grant. DoD funding for this research ended in September 2012, however, due to the expected significance of these experiments, we will continue the investigative work as proposed in this grant proposal under a different funding source.

KEY RESEARCH ACCOMPLISHMENTS

1. We have extensively characterized the phosphorylation of ZMYND8 after different types of DNA damage and replication stress **(SOW Tasks 1 a-d)**, as well as the requirement of ATM and ATR kinases for this phosphorylation **(Milestone #1)**
2. We have discovered a potential therapeutic target in ZMYND8 serine1060, where ZMYND8 is rapidly and strongly phosphorylated when cells are exposed to replication stress **(SOW Task 1.b)**
3. We have performed mechanistic studies on the biological function of ZMYND8 in the survival following genotoxic stress **(SOW Task 1e)** and have submitted a publication of these finding **(Milestone #2)**.
4. ZMYND8/RACK7 is overexpressed in BRCA1 mutant mouse mammary tumors **(SOW Task 2)**
5. RACK7 overexpressing transgenic mice are being genotyped. **(SOW Task 3a)**
6. The shRNA targeting mouse ZMYND8 has been validated upon adjustment from the original proposed shRNA sequence. A mere 48 hours after transfection with shRNA yields significantly knocked-down ZMYND8. **(SOW Task 3b)**

REPORTABLE OUTCOMES

We have characterized ZMYND8 as a novel factor of genomic stability. We found that ZMYND8 is phosphorylated after replication stress and DNA damage. ZMYND8 is frequently overexpressed in cancer and elevated levels of ZMYND8 can protect cancer cells from replication stress. We have presented these findings at the 2012 Maintenance of Genome Stability conference. A manuscript describing our findings has been submitted for publication in Nature and is attached in the appendix of this report. The final paper attached to this report describes the original screen discovering RACK7/ZMYND8 and potential involvement in BRCA1-mediated DNA damage pathway.

Abstract:

"The Novel Zinc-finger Protein ZMYND8 Is Involved in the Stabilization of Stalled Replication Forks", Martin Preyer and Inder M. Verma (2012), Maintenance of Genome Stability Conference

Publications:

"ZMYND8 protects cancer cells against replication stress through stabilization of stalled forks", Martin Preyer and Inder M. Verma (2012), Nature, *submitted*

*"*A genetic screen identified RACK7 as a novel factor involved in BRCA1-mediated DNA damage sensitivity pathway", Quan Zhu et al., (2012) *in preparation* (attached in appendix)

CONCLUSIONS

The work funded by this grant has led to the discovery of ZMYND8 as a novel factor involved in maintaining genomic stability. Our results provide evidence that overexpression of ZMYND8 in breast and ovarian cancer, as well as in several other malignancies, is a novel mechanism to overcome replication stress. This significant and novel finding demonstrates that ZMYND8 is required to prevent the reversal of stalled replication forks, and thereby contributes to genomic stability under replication stress. It is interesting to note that a recent proteomics study on the co-regulator interactome [13] has indicated that ZMYND8 may be associated with histonemodifying enzymes. It is well known that histone modification and chromatin remodeling are an integral part of the DNA damage response [18], since chromatin needs to be decondensed and nucleosomes (re-)moved to grant access of repair factors [19-21]. Thus, ZMYND8 may be linked to the chromatin de-condensation, nucleosome sliding, and histone modification at the sites of DNA damage. While chromatin is already de-condensed and histones unloaded at the replication fork, the histone H2AX nevertheless becomes phosphorylated in the vicinity when a replication fork stalls [22]. Our data indicate that ZMYND8 might be involved in the chromatin reorganization surrounding a stalled fork, which may be vital in preventing the collapse and and granting genomic stability. Furthermore, our data suggest that ZMYND8 and BRCA1 function epistatic in the recovery of stalled replication forks. It is interesting to mention, that a recent publication reported that BRCA1 is required for the repair of forks stalled by UV-induced photoadducts [23]. However, the molecular function of BRCA1 and ZMYND8 at stalled replication forks and its importance to genomic stability are unknown. Mechanistic insights on the functions of ZMYND8 and BRCA1 during replication stress will increase our understanding of fork stalling and its role in carcinogenesis. We believe the *in vivo* studies are critical to our understanding of BRCA1 and ZMYND8 epistatic function in disease, and therefore we will continue to study the effects of ZMYND8 and BRCA1 with respect to breast cancer.

REFERENCES

1. Narod, SA and Foulkes, WD. *BRCA1 and BRCA2: 1994 and beyond.* Nat Rev Cancer, 2004. 4(9): p. 665-76.
2. Venkitaraman, AR. *Functions of BRCA1 and BRCA2 in the biological response to DNA damage.* J Cell Sci, 2001. 114(Pt 20): p. 3591-8.
3. Moynahan ME, Chiu JW, Koller BH, Jasin M. *Brca1 controls homology-directed DNA repair.* Mol Cell, 1999. 4(4): p. 511-8.
4. Moynahan, ME, AJ Pierce, and M Jasin, *BRCA2 is required for homology-directed repair of chromosomal breaks.* Mol Cell, 2001. 7(2): p. 263-72.
5. Scully R, Chen J, Ochs RL, Keegan K, Hoekstra M, Feunteun J, Livingston DM. *Dynamic changes of BRCA1 subnuclear location and phosphorylation state are initiated by DNA damage.* Cell, 1997. 90(3): p. 425-35.
6. Scully R, Ganesan S, Vlasakova K, Chen J, Socolovsky M, Livingston DM. *Genetic analysis of BRCA1 function in a defined tumor cell line.* Mol Cell, 1999. 4(6): p. 1093-9.
7. Zhong Q, Chen CF, Li S, Chen Y, Wang CC, Xiao J, Chen PL, Sharp ZD, Lee WH. *Association of BRCA1 with the hRad50-hMre11-p95 complex and the DNA damage response.* Science, 1999. 285(5428): p. 747-50.
8. Yang H, Jeffrey PD, Miller J, Kinnucan E, Sun Y, Thoma NH, Zheng N, Chen PL, Lee WH, Pavletich NP. *BRCA2 function in DNA binding and recombination from a BRCA2-DSS1-ssDNA structure.* Science, 2002. 297(5588): p. 1837-48.
9. Chen L, Nievera CJ, Lee AY, Wu X. *Cell cycle-dependent complex formation of BRCA1.CtIP.MRN is important for DNA double-strand break repair.* J Biol Chem, 2008. 283(12): p. 7713-20.
10. Coleman, KA and Greenberg, RA. *The BRCA1-RAP80 complex regulates DNA repair mechanism utilization by restricting end resection.* J Biol Chem, 2011. 286(15): p. 13669-80.
11. Bunting SF, Callén E, Wong N, Chen HT, Polato F, Gunn A, Bothmer A, Feldhahn N, Fernandez-Capetillo O, Cao L, Xu X, Deng CX, Finkel T, Nussenzweig M, Stark JM, Nussenzweig A. *53BP1 inhibits homologous recombination in Brca1-deficient cells by blocking resection of DNA breaks.* Cell, 2010. 141(2): p. 243-54.
12. Yun, M.H and Hiom, K. *CtIP-BRCA1 modulates the choice of DNA doublestrand-break repair pathway throughout the cell cycle.* Nature, 2009. 459(7245):
p. 460-3.
13. Malovannaya A, Lanz RB, Jung SY, Bulynko Y, Le NT, Chan DW, Ding C, Shi Y, Yucer N, Krenciute G, Kim BJ, Li C, Chen R, Li W, Wang Y, O'Malley BW, Qin J. *Analysis of the human endogenous coregulator complexome.* Cell, 2011. 145(5): p. 787-99.
14. Spellman, P. T., et al. *Integrated genomic analysis of ovarian carcinoma.* Nature, 2011, 474, 609–615.
15. Matsuoka S, Ballif BA, Smogorzewska A, McDonald ER 3rd, Hurov KE, Luo J, Bakalarski CE, Zhao Z, Solimini N, Lerenthal Y, Shiloh Y, Gygi SP, Elledge SJ. *ATM and ATR substrate analysis reveals extensive protein networks responsive to DNA damage.* Science, 2007. 316(5828): p. 1160-6.
16. Anantha, RW, Vassin, VM, Borowiec, JA. *Sequential and synergistic modification of human RPA stimulates chromosomal DNA repair.* J Biol Chem, 2007. 282(49): p. 35910-23.
17. Lukk, M, Kapushesky, M, Nikkilä, J, Helen Parkinson, H, Goncalves, A, Huber, W,Ukkonen, E, Brazma, A. *A global map of human gene expression*. Nature Biotechnology 2010, 28, 322–324.
18. Misteli, T and Soutoglou, E. *The emerging role of nuclear architecture in DNA repair and genome maintenance.* Nat Rev Mol Cell Biol, 2009. 10(4): p. 243-54.
19. Goodarzi AA, Noon AT, Deckbar D, Ziv Y, Shiloh Y, Löbrich M, Jeggo PA. *ATM signaling facilitates repair of DNA double-strand breaks associated with heterochromatin.* Mol Cell, 2008. 31(2): p. 167-77.
20. Murr R, Loizou JI, Yang YG, Cuenin C, Li H, Wang ZQ, Herceg Z. *Histone acetylation by Trrap-Tip60 modulates loading of repair proteins and repair of DNA double-strand breaks.* Nat Cell Biol, 2006. 8(1): p. 919.
21. Noon AT, Shibata A, Rief N, Löbrich M, Stewart GS, Jeggo PA, Goodarzi AA. *53BP1-dependent robust localized KAP-1 phosphorylation is essential for heterochromatic DNA double-strand break repair.* Nat Cell Biol, 2010. 12(2): p. 177-84.

22. Ward, I.M and Chen, J. *Histone H2AX is phosphorylated in an ATR-dependent manner in response to replicational stress.* J Biol Chem, 2001. 276(51): p. 47759-62.
23. Pathania S, Nguyen J, Hill SJ, Scully R, Adelmant GO, Marto JA, Feunteun J, Livingston DM. *BRCA1 is required for postreplication repair after UV-induced DNA damage.* Mol Cell, 2011. 44(2): p. 235-51.

APPENDICES

Supportive Information: Figures 1-7

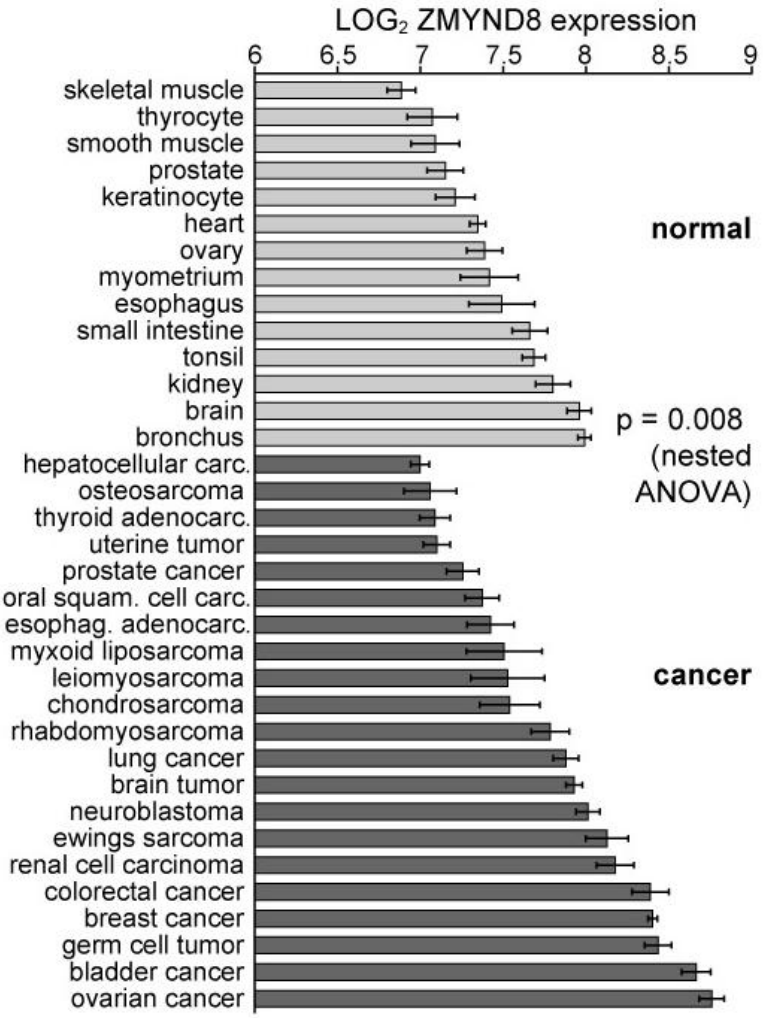

Figure 1. ZMYND8 expression in normal and cancer tissues. ZMYND8 expression was analyzed in a consistently normalized set of data from the gene expression atlas. Log_2 transformed expression levels of ZMYND8 in 1600 samples from cancers and normal tissues are shown (mean +/- s.e.m.) A nested ANOVA was performed to analyze the variance of ZMYND8 expression between normal tissues and cancer.

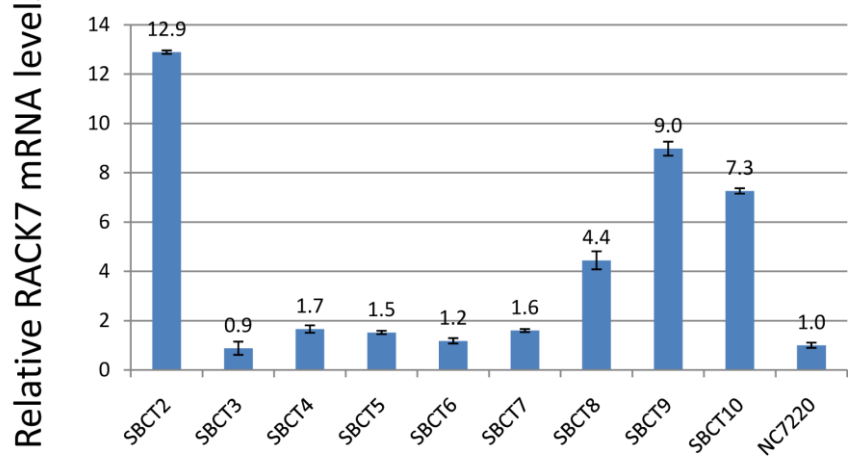

Figure 2. Realtime PCR experiment to measure the expression levels of RACK7 in human breast tumors. RNA samples were isolated from 9 tumors (SBCT2 to 10) and a normal mammary tissue (NC7220). The relative expression levels of RACK7 were normalized by that of GAPDH.

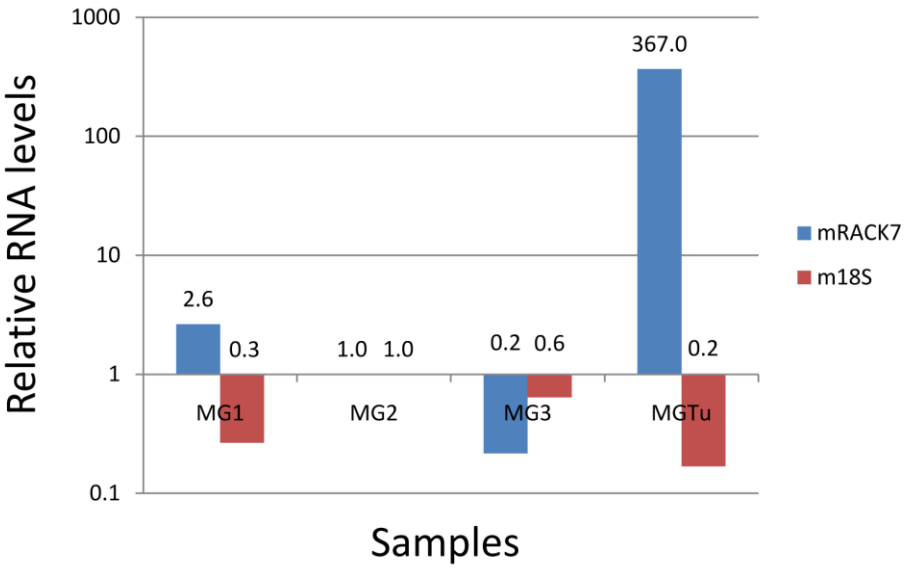

Figure 3. Realtime PCR experiment to measure the expression levels of RACK7 in BRCA1-deficient mouse tumors. RNA samples were isolated from BRCA1-deficient mouse tumor (MGTu) and mammary glands from age-matched wildtype litter-mates (MG1, MG2 and MG3). The relative expression levels of RACK7 were normalized by that of cyclophylin.

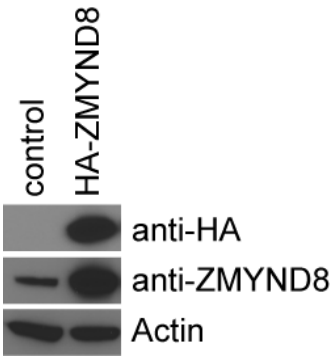

Figure 4. Western blotting to detect the expression of HA tagged ZMYND8/RACK7 in cultured cells. The protein can be detected by both HA tag and the RACK7 antibody.

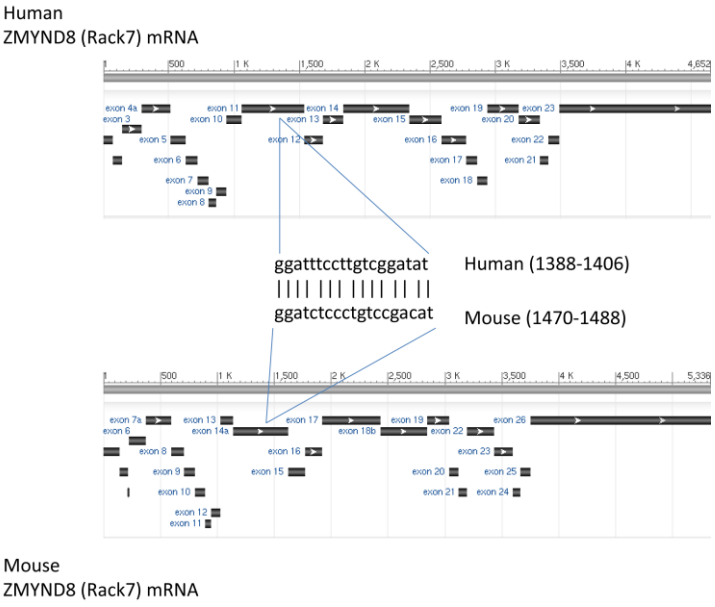

Figure 5. The sequence of shRNA targeting mouse RACK7 as shown in the context of its genomic loci.

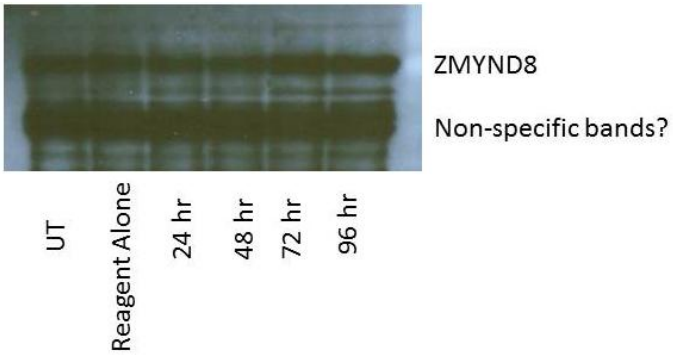

Figure 6. Western Blot analysis of transfected MEFs with original mouse shRNAto ZMYND8. Transfection was facilitated by lipofectamine, and indicated control Reagent alone is lipofectamine alone. Protein was isolated at 24, 48, 72 and 96 hours post transfection. ZMYND8 antibody detects corresponding ZMYND8 band at 131kDa and dominant non-specific bands at 80 and 90 kDa.

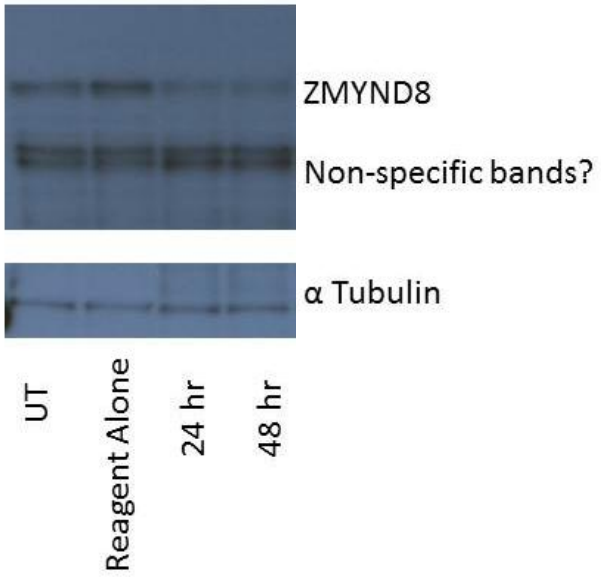

Figure 7. Western Blot analysis of transfected MEFs with new shRNA generated from Open Biosystems to mouse ZMYND8. Transfection was facilitated by lipofectamine, and indicated control Reagent alone is lipofectamine alone. Protein was isolated at 24 and 48, hours post transfection. ZMYND8 antibody detects corresponding ZMYND8 band at 131kDa and dominant non-specific bands at 80 and 90 kDa. Tubulin was used as a loading control.

ZMYND8 protects cancer cells against replication stress through stabilization of stalled forks

Martin Preyer and Inder M. Verma

Laboratory of Genetics, The Salk Institute for Biological Studies, La Jolla, California 92037, USA.

running title: Reversal of replication forks

Keywords: ZMYND8, ATR, replication stress, hydroxyurea, fork restart, fork reversal, chicken foot, ionizing radiation, DNA fiber assay

correspondence should be addressed to:

Inder Verma

Laboratory of Genetics

The Salk Institute

10010 North Torrey Pines Road

La Jolla, CA 92037

tel. 858-453-4100 x1462

e-mail: verma@salk.edu

SUMMARY PARAGRAPH

Activation of oncogenes and rapid progression through the cell cycle cause replication stress in cancer cells, an impediment to fast growth[1-3]. Thus, tumors must develop means to evade or overcome replication stress[4]. The gene *zmynd8*, whose biological function is unknown, was recently found significantly amplified in ovarian cancer by The Cancer Genome Atlas (TCGA) research network[5]. Here we show that ZMYND8 is phosphorylated by ATR to stabilize stalled replication forks and increase cell survival following replication stress. Using single-molecule DNA fiber assays, we found that stalled forks are reversed in cells lacking ZMYND8 causing a delayed restart after stress. Interestingly, the repair of reversed forks during prolonged stalling leads to aberrant restart and creates extensive single-stranded DNA. Thus, fork reversal poses a threat to genomic stability, revising the notion that reversal is an intermediate of fork restart[6,7]. Analysis of gene expression data revealed frequent overexpression of ZMYND8 in cancer, lending support to the hypothesis that elevated levels of ZMYND8 can protect cells during replication stress. Indeed, overexpressed ZMYND8 accumulated at forks and increased the cell survival following nucleotide depletion. We conclude that ZMYND8 amplification in cancer is a novel mechanism to overcome replication stress.

MAIN TEXT

Unwinding and semiconservative replication of the parental DNA occurs in a highly coordinated fashion at replication forks. The progression of a replication fork can stall when the replisome collides with transcription complexes, with secondary structures or damaged DNA, or when deoxynucleotides become rate-limiting[8-10]. A common feature of stalled forks is single-stranded DNA (ssDNA), which is bound by the conserved replication protein A (RPA) leading to the activation of the ATM and Rad3-related (ATR) kinase[11]. ATR then acts as central signal transducer in the replication stress response[12,13]. Stalled replication forks are stabilized by a complex involving Claspin, Tim1 and Tipin[14], but several lines of evidence suggest that stalled forks undergo changes over time. In yeast, the reversal of forks into a Holliday junction termed "chicken foot" has been observed in the absence of the checkpoint effector Rad53[15]. The recombination protein RAD51 and other repair proteins accumulate at forks after several hours of stalling[16,17], which is thought to facilitate recombination-dependent repair and restart[7,18]. RAD51 has also been reported to antagonize the degradation of the nascent strands by MRE11 during stalling[19]. Eventually, stalled forks may be cleaved by the MUS81 endonuclease and DNA replication is completed by the firing of dormant origins[20,21]. Altogether, neither the mechanism of fork stabilization nor the events occurring during stalling are well understood.

The zinc finger MYND-type containing 8 (ZMYND8) protein is predicted to contain several domains (Fig. 1a): a PHD-type zinc finger, which may associate with methylated histones; a Bromodomain that can bind acetyl-lysine; a Pro-Trp-Trp-Pro (PWWP)

domain, which also binds methylated histones[22]; and a MYND-type zinc finger, which can mediate protein-protein interactions. Databases of NCBI and ENSEMBL list several transcript variants of ZMYND8. In western blots we found ZMYND8 expressed as a single band in several cell types, which co-migrated with ectopically expressed ZMYND8 (Fig. 1b and Supplementary Fig. S1a-c). Multiple domains of ZMYND8 suggest an interaction with chromatin and the protein has been found in complexes with histones, chromatin remodeling and transcription complexes[23]. In immunostainings we found that ZMYND8 is exclusively nuclear (Supplementary Fig. S1d) and subcellular fractionation experiments confirmed that the majority of the protein is associated with chromatin (Supplementary Fig. S1e).

The phosphorylation of ZMYND8 at an ATM/ATR consensus site after ionizing radiation (IR) has been identified by a phospho-proteomics study[24]. We were able to detect this phosphorylation by immunoprecipitating ZMYND8 followed by western blotting with an ATM-substrate antibody (anti phospho-SQ; Supplementary Fig. S2a). The phosphorylation was ATM-dependent (Fig. S2b), but occurred only at late time points after high doses of IR (Supplementary Fig. S2c,d), suggesting that ZMYND8 is not involved in the early steps of double-strand break repair. Consistent with this notion, we found that the knockdown of ZMYND8 did not significantly alter the survival after IR (Supplementary Fig. S2e &f). We therefore tested whether ZMYND8 might play a role in response to other types of genotoxic stress. Interestingly, we found that the phosphorylation of ZMYND8 was induced following nucleotide depletion with hydroxyurea (HU) likely due to replication stress. In fact, it was detectable following

partial inhibition of ribonucleotide reductase with a low dose of HU (Fig. 1c). A time course revealed that ZMYND8 phosphorylation occurs rapidly in response to replication stress, similar to the phosphorylation of CHK1 and γH2AX (Fig. 1d). The phosphorylation of ZMYND8 after HU was blocked by mutation of serine 1060 to alanine (Fig. 1e), suggesting that the same serine is phosphorylated after IR (Supplementary Fig. S2a) and replication stress. This raised the question, whether phosphorylation following HU treatment is also ATM-dependent, since ATR and not ATM is the major signal transducer of replication stress[12]. We found that HU-induced phosphorylation of ZMYND8 was sensitive to caffeine, which inhibits ATR kinase activity[25], but insensitive to the ATM inhibitor KU55933 (Fig. 1f). Thus, serine 1060 of ZMYND8 is phosphorylated rapidly by ATR in response to nucleotide depletion. Next, we determined the HU sensitivity of cells in clonogenic survival assays. When we knocked down ZMYND8 using two different shRNAs (Fig. 1g), cells became sensitive to HU and formed significantly fewer colonies compared to control cells expressing an shRNA against luciferase (Fig. 1h, i). Thus, ZMYND8 is required for the survival of HU-induced replication stress. Cells lacking ZMYND8 were also sensitive to aphidicolin (Fig. 1j), which directly inhibits the replicative DNA polymerases. To confirm that the HU sensitivity was due to the lack of ZMYND8, we re-expressed an shRNA-resistant ZMYND8 in knockdown cells at a similar level compared to the endogenous protein (Supplementary Figure S3). Wild-type ZMYND8 rescued the survival after HU treatment, but re-expression of the S1060A-mutant, which cannot be phosphorylated by ATR, did not rescue HU sensitivity (Fig. 1k), demonstrating that the phosphorylation of ZMYND8 is necessary for cell survival.

To investigate the stalling and restart of replication forks we performed DNA fiber assays, in which nascent DNA is labeled by the incorporation of 5-iododeoxyuridine (IdU) and 5-chlorodeoxyuridine (CldU) before and after stalling, respectively. Thus, the progression of individual replication forks can be visualized by immunostaining of single-molecule DNA fibers. In these experiments, control cells and ZMYND8 knockdown cells showed similar fork progression before stalling (green IdU tracks in Fig. 2a; median 8.22 vs. 8.61 μm). Control cells were able to swiftly restart forks after HU removal, as evident from the red CldU tracks adjacent to green tracks in Figure 2a. ZMYND8 knockdown cells, however, showed significantly shorter CldU tracks (median 1.86 μm vs. 4.24 μm, $p = 1.03 \times 10^{-26}$). This suggests that replication restart in ZMYND8 knockdown cells was either delayed or forks progressed slower after restart. Measuring the track lengths later after restart demonstrated that forks proceeded with similar speed in knockdown and control cells (Fig. 2b). At an earlier time point, when most forks in control cells had incorporated CldU (Fig. 2c), there was little fork restart evident in ZMYND8 knockdown cells, suggesting that restart is delayed. The delayed restart was rescued by wildtype ZMYND8 but not by the phosphorylation site-mutant S1060A (Fig. 2d), demonstrating again the requirement for ZMYND8 phosphorylation.

To investigate whether the delayed fork restart in ZMYND8 knockdown cells was due to defects during stalling, we prepared DNA fibers directly from HU-stalled cells without restart. As expected, the replication tracks of control cells showed rather constant intensity along the track (Fig. 3a). In contrast, the replication tracks of cells lacking

ZMYND8 showed a drumstick morphology with increased intensity at one end (Fig. 3a). Sequential labeling with CldU and IdU confirmed that the tip of the drumsticks corresponded to the most recently replicated DNA, i.e. the fork (Suppl. Fig. S4). Measuring the fluorescence intensity along individual tracks, we found a significant increase in intensity at the tip of approximately half the tracks of ZMYND8 knockdown cells compared to 10-15% in the control (Fig. 3b). The increase in intensity at the tip of the drumsticks was 1.8-fold, suggesting that double the amount of IdU-labeled nascent DNA is present (Suppl. Fig. S4). This indicates that stalled forks in ZMYND8 knockdown cells are reversed or remodeled and thus the linear configuration is altered. To confirm that the drumstick shape is indeed caused by regression, we performed a sequential labeling with a short 2-minute pulse of IdU before stalling. In control cells, the tracks showed the expected sequential appearance of a short green IdU signal adjacent to a red CldU track (Fig. 3c). However, the IdU and CldU signals overlaid or appeared reversed in drumstick-shaped tracks of ZMYND8 knockdown cells (Fig. 3c, yellow, due to merge of green IdU and red CIdU signals), providing a direct evidence for the reversal of stalled forks.

Next, we used a recently developed method for the isolation of proteins on nascent DNA (iPOND)[17], which labels nascent DNA with 5-ethynyl-2'-deoxyuridine (EdU) followed by biotinylation using click-chemistry. Using a streptavidine-pulldown, we detected ZMYND8 in unstressed cells both in the vicinity of replication forks and at downstream chromatin (Fig. 3d). This suggests that ZMYND8 might function in chromatin-related processes during replication, possibly being involved in the re-establishment of

chromatin structure behind the fork. The treatment with HU did not change the amount of ZMYND8 near forks (Fig. 3e). Interestingly, the sliding clamp PCNA remained associated with the fork during one hour stalling. This could explain the ability to swiftly restart replication after HU removal. However, in cells lacking ZMYND8, which displayed fork reversal, the recombination protein RAD51 was recruited to HU-stalled forks (Fig. 3e). This confirms that ZMYND8 maintains the integrity of stalled forks by preventing reversal or recombination events. As a consequence, forks in knockdown cells cannot swiftly resume replication when nucleotide pools are replenished after HU-removal.

The events occurring during fork stalling and restart are largely unknown. During extended stalling, the fork integrity might be lost[16], leading to the processing by nucleases[19-21,26]. Consistent with this notion, we found that the toxicity of HU was strongly dependent on exposure time. Short stalling had no effect on the clonogenic survival, but HU-stalling for several hours led to toxicity, which was more extensive in ZMYND8 knockdown cells (Fig. 4a). This result suggests that the fork reversal and delayed restart in ZMYND8 knockdown cells after short stalling (Figures 2 and 3) do not affect viability. Thus, we depleted nucleotides for several hours to investigate fork restart under these conditions. Interestingly, cells retained the ability to restart forks after 5 hours stalling with 1 mM HU (Fig. 4b). However, the red CldU and green IdU tracks were not immediately adjacent under these conditions, and the gap between CldU and IdU was greatly extended in ZMYND8 knockdown cells (Fig. 4b). Shortening the time of HU exposure reduced the gap size, confirming that the gaps resulted from fork

movement during stalling rather than firing of nearby origins (Supplementary Fig. S5). Because the repair and restart of collapsed forks has been proposed to function via recombination[7,27] and we had observed the recruitment of the recombination protein RAD51 to stalled forks in ZMYND8 knockdown cells (Fig. 3e lane 4), we hypothesized that this fork movement is a result of aberrant recombination and restart. To test this hypothesis, we added CldU to the media during HU-stalling to monitor nucleotide incorporation. We detected little CldU incorporation in control cells, but significantly longer CldU tracks in ZMYND8 knockdown cells (Fig. 4c). This suggests that the fork movement results from restart and at least partial DNA synthesis. The CldU incorporation during HU was completely blocked by aphidicolin (Suppl. Fig. S5), which inhibits replicative polymerases but not translesion polymerases, ruling out the possibility of erroneous polymerase switching. Thus, fork reversal and RAD51 recruitment in cells lacking ZMYND8 lead to aberrant restart of stalled forks. As a consequence of the aberrant restart, which could cause repetitive stalling, ZMYND8 knockdown cells developed regions of ssDNA, which we detected by BrdU staining under non-denaturing conditions (Fig. 4d). ZMYND8 knockdown cells also formed RPA foci during HU treatment (Suppl. Fig. 6), confirming that extensive regions ssDNA were created by partial or hemi-replication[15]. The aberrant restart was, however, not due to a defect in checkpoint activation, because ZMYND8 knockdown cells showed normal phosphorylation of CHK1 (Supplementary Fig. S7). This result also implies that upstream events required for CHK1 activation, such as RAD17 phosphorylation[28], loading of the 9-1-1 clamp, and CLASPIN phosphorylation[12,13,29] do not require ZMYND8.

Because the *zmynd8* gene is frequently amplified in ovarian cancer[5], we analyzed ZMYND8 expression levels in a variety of cancers and normal tissues using consistently normalized data[30] from the gene expression atlas (http://www.ebi.ac.uk/gxa). In accordance with the frequent amplification, ZMYND8 expression was highest in ovarian cancer ($p = 4.7\times10^{-9}$ vs. normal ovary, Suppl. Fig. S8). Interestingly, ZMYND8 was also highly expressed in several other cancers, including bladder, germ cell, breast and colorectal cancers. Analysis of the expression across the dataset by nested ANOVA revealed that ZMYND8 is significantly higher expressed in cancer compared to normal tissues ($p = 0.008$). Because our results suggest that ZMYND8 protects the integrity of stalled forks, we hypothesized that increased levels of ZMYND8 may confer resistance to replication stress. Using a lentiviral vector with a strong promoter (CMV/chicken beta-actin) to overexpress ZMYND8 (Fig. 5a), we found that cells became significantly resistant to nucleotide depletion (Fig. 5b). The overexpression of ZMYND8 also led to accumulation of the protein near replication forks (Fig. 5c), suggesting that normal ZMYND8 levels are limiting. These results demonstrate that elevated levels of ZMYND8 can protect stalled replication forks, and that ZMYND8 overexpression is therefore beneficial for the rapid proliferation of cancer cells.

Altogether, our results support a model (Fig. 5d) in which ZMYND8 is rapidly phosphorylated by ATR after nucleotide depletion to prevent fork reversal. The reversal of forks by pairing of the two nascent strands was discovered many years ago[31,32], but it is still unclear whether it represents a normal step towards restart or a product of fork collapse requiring repair[6]. Our results provide evidence for the latter, since the reversal of forks and recruitment of RAD51 correlated with a delayed restart in cells lacking ZMYND8, whereas control cells showed swift restart without apparent RAD51 recruitment. It is currently not clear, which forces drive the regression of stalled forks. Positive supercoiling ahead of the fork[33] as well as several helicases, which are involved in replication stress[7], could be contributing factors. ZMYND8 seems to counteract these forces and prevent regression. Consequently, in cells expressing ZMYND8, the recombination protein RAD51 does not accumulate rapidly at stalled forks, which has also been observed by two recent studies[16,17]. Interestingly, we also found that cell survival was not affected by short stalling nor by the fork reversal in ZMYND8 knockdown cells during short stalling. Instead, cell survival decreased only after prolonged stalling, suggesting that aberrant recombination or restart contribute to toxicity. This hypothesis is supported by the fact that MUS81 endonuclease, which can cleave Holliday junctions and replication intermediates following stalling[20], has been found to limit cell death after oncogene-induced replication stress[34]. The present study demonstrates that rapid stabilization of stalled forks by ZMYND8 is an early response to limit such toxic recombination events.

METHODS

Cells culture and DNA damaging agents

All cell lines were grown in DMEM supplemented with 10% FBS and penicillin/streptomycin antibiotics (Invitrogen). KU55933 was purchased from Calbiochem. HU, aphidicolin, and caffeine were from Sigma. Gamma irradiations were done using an irradiator with a ^{60}Co source.

Cloning of ZMYND8

We cloned the N-terminus of ZMYND8 from mRNA of 293T cells using standard cloning methods, and fused this fragment, using a unique XmaI site, to the cDNA clone 4844473 (Open Biosystems), which lacks the N-terminal 281 base pairs of the coding region. Sequencing of the complete cDNA confirmed identity with the NCBI Reference Sequence NM_183047.1 of ZMYND8 transcript variant 1. All point mutations and epitope tags were created using standard PCR-based mutagenesis techniques, and all amplified regions were sequenced for amplification errors and correctness of mutations.

Western blotting and Immunoprecipitation

Cells were lysed in RIPA buffer (50 mM Tris/HCl pH7.4, 150 mM NaCl, 1 mM EDTA, 1 mM EGTA, 1% NP-40, 0.25% sodium deoxycholate, 0.1% SDS) supplemented with complete protease inhibitor (Roche) and Halt phosphatase inhibitor (Pierce), or by boiling in 1x LDS sample buffer (Invitrogen) followed by sonication. The antibodies used were monoclonal ZMYND8 (Santa Cruz) and polyclonal ZMYND8 (Sigma), CHK2 pS28

(Abcam) to detect ZMYND8 phosphorylation, monoclonal HA.11 (Covance), phospho-H2AX clone JBW301 (Millipore), PCNA and RAD51 (Santa Cruz Biotech), rabbit monoclonal CHK1 pS317 and pS345, and polyclonal mTor, H3, pan-Actin, CHK2 pT68, total CHK2 and CHK1 (all from Cell Signaling). For immunoprecipitations, samples were incubated with 1 μg of anti-HA or 3 μg of polyclonal anti-ZMYND8 for 1-2 hours, followed by pull-down with protein G fast-flow beads (Amersham) for 1-2 hours at 4ºC. Beads were washed three times with RIPA buffer, and samples eluted by boiling in LDS sample buffer.

iPOND

EdU-labeling and pulldown were done, with minor modifications, as previously described[17]. Briefly, 5×10^7 cells were labeled with 40 μM EdU (Invitrogen), fixed with 1 % PFA for 10-15 minutes, and the fixation quenched by the addition of 1/20th volume 2.5 M glycine. Cells were washed, harvested and frozen at -80ºC. Cells were permeabilized in 0.25% Triton X-100 in PBS, washed, and biotinylated with 4 μM biotin-azide in 1 ml Click-it reaction buffer (Invitrogen) according to the manufacturers instructions. After washing in PBS, cells were lysed in 50 μM Tris/HCl with 1 % SDS containing protease inhibitors, and chromatin sheared by 4 pulses of 15 seconds at 40% amplitude with an ultrasonic processor (Cole Palmer). Insoluble material was removed by centrifugation at 21000 g, and biotin complexes purified over night at 4 ºC on 40 μl streptavidine agarose (Invitrogen). Beads were washed twice with lysis buffer, once with 1 M NaCl, and twice with lysis buffer, and complexes eluted and reverse crosslinked by boiling in LDS sample buffer.

Cell fractionation

Cytoplasma was extracted in hypotonic buffer (10 mM HEPES, 50 mM NaCl, 0.5% Triton X-100, 0.3 M sucrose) on ice for 10 min, nuclei were spun down at 1500 g for 5 min and washed in hypotonic buffer. Soluble nuclear proteins were extracted in high salt buffer (10 mM HEPES, 200 mM NaCl, 1 mM EDTA, 0.5% NP-40) on ice for 10 min and cleared from the insoluble chromatin fraction at 21000 g for 5 minutes. The chromatin fraction was sonicated after boiling in LDS sample buffer to shear DNA.

shRNA knockdown

The shRNAs against the target sequences ZMYND8 (#1) 5'-GGATTTCCTTGTCGGATAT-3', ZMYND8 (#2) 5'-GCATCGAGACCCAGAGTAA-3', and Luciferase 5'-GTGCGCTGCTGGTGCCAAC-3' were expressed in lentiviral vectors under the human H1 promoter. Lentivirus was produced in 293T cells following standard protocols. U2OS cells were infected with virus-containing supernatant on two consecutive days and allowed to recover for 2 to 4 passages before being used in experiments. The sh-resistant ZMYND8 was created by mutating the targeted sequence to 5'-G<u>C</u>AT<u>AAG</u>CTTGTC<u>T</u>GATA-3' (mutated bases are underlined).

Clonogenic survival assay

U2OS cells (500-1000) were seeded in 6-cm culture dishes, allowed to adhere for 16 hours, and treated for 24 hours or as indicated. Drugs were removed by washing with PBS and cells grown in media for 8-10 days to form colonies. Cells were fixed in methanol at -20ºC and stained with 0.5% crystal violet in 20% methanol. Dishes were

scanned, and colonies (>50 cells) counted using ImageJ software. Clonogenic survival is given as percentage of respective untreated controls.

DNA fiber assay

Cells were labeled in media containing 10 μg/ml of IdU or CldU (Sigma) for the indicated time. Harvesting, lysis, DNA fiber spreading on glass slides and fixation was done as described previously[16]. After denaturation with 2.5 M HCl for 1 hour, slides were blocked 3% BSA in PBS containing 0.1% Tween 20. Immunofluorescent staining was done with the BrdU antibodies B44 (Becton Dickinson; mouse monoclonal, recognizes IdU) and BU1/75 (Novus; rat monoclonal, recognizes CldU) at 1:200 dilution for 2 hours. Anti-mouse Alexa488 and anti-rat Alexa564 (Molecular Probes) were used at 1:1000, slides were mounted using Fluorogel (Electron microscopy Sciences), and images taken on LSM 710 or LSM 780 confocal microscopes (Zeiss). For the analysis of replication track lengths, around 100 individual tracks from several images were measured using ImageJ software. Fluorescence intensity along tracks was also measured by ImageJ.

Immunofluorescence

U2OS cells were seeded on cover slips and allowed to adhere over night before HU treatment. Cells were fixed with 4% paraformaldehyde in PBS and blocked with 5% goat serum in PBS. Staining was done using antibodies γH2AX and RPA32 (Bethyl Laboratories). DNA was counterstained with Hoechst 33258.

Statistical analysis

Unpaired two-sided Student's t-tests were performed as indicated in the figure legends. DNA fiber lengths were compared by Mann-Whitney U tests. The gene expression data set from 5,372 human samples and its normalization have been described[30]. In our analysis, we included only groups that contain more than 5 samples, and averaged across the ZMYND8 probes for each sample. In the case of dependent groups, we included only the more broadly defined group (e.g. brain but not cortex) in our analysis. Blood and hematological malignancies were excluded because of multiple dependent categories in the dataset (e.g. B-cell, lymphocyte, leukocyte, blood). Samples from non-adult tissues were excluded to avoid any developmental bias. We did not include data from cell lines and diseases other than cancer in our analysis, resulting in a final set of 1600 samples in 14 normal subgroups and 21 cancer subgroups shown in Supplementary Figure S8. A nested ANOVA was performed showing significant variance between subgroups $p = 3.79\times10^{-122}$ (with $F_{33, 1565} = 25.57$) and between the groups cancer versus normal, $p = 0.008$ (with $F_{1, 33} = 7.97$).

REFERENCES

1. Bartkova, J.*, et al.* Oncogene-induced senescence is part of the tumorigenesis barrier imposed by DNA damage checkpoints. *Nature* **444**, 633-637 (2006).
2. Di Micco, R.*, et al.* Oncogene-induced senescence is a DNA damage response triggered by DNA hyper-replication. *Nature* **444**, 638-642 (2006).
3. Bester, A.C.*, et al.* Nucleotide deficiency promotes genomic instability in early stages of cancer development. *Cell* **145**, 435-446 (2011).
4. Halazonetis, T.D., Gorgoulis, V.G. & Bartek, J. An oncogene-induced DNA damage model for cancer development. *Science* **319**, 1352-1355 (2008).
5. The Cancer Genome Atlas Research Network. Integrated genomic analyses of ovarian carcinoma. *Nature* **474**, 609-615 (2011).
6. Atkinson, J. & McGlynn, P. Replication fork reversal and the maintenance of genome stability. *Nucleic Acids Res* **37**, 3475-3492 (2009).
7. Petermann, E. & Helleday, T. Pathways of mammalian replication fork restart. *Nat Rev Mol Cell Biol* **11**, 683-687 (2010).
8. Gomez-Gonzalez, B.*, et al.* Genome-wide function of THO/TREX in active genes prevents R-loop-dependent replication obstacles. *EMBO J* **30**, 3106-3119 (2011).
9. Deshpande, A.M. & Newlon, C.S. DNA replication fork pause sites dependent on transcription. *Science* **272**, 1030-1033 (1996).
10. Azvolinsky, A., Giresi, P.G., Lieb, J.D. & Zakian, V.A. Highly transcribed RNA polymerase II genes are impediments to replication fork progression in Saccharomyces cerevisiae. *Mol Cell* **34**, 722-734 (2009).

11. Zou, L. & Elledge, S.J. Sensing DNA damage through ATRIP recognition of RPA-ssDNA complexes. *Science* **300**, 1542-1548 (2003).

12. Cimprich, K.A. & Cortez, D. ATR: an essential regulator of genome integrity. *Nat Rev Mol Cell Biol* **9**, 616-627 (2008).

13. Paulsen, R.D. & Cimprich, K.A. The ATR pathway: fine-tuning the fork. *DNA Repair (Amst)* **6**, 953-966 (2007).

14. Chou, D.M. & Elledge, S.J. Tipin and Timeless form a mutually protective complex required for genotoxic stress resistance and checkpoint function. *Proc Natl Acad Sci U S A* **103**, 18143-18147 (2006).

15. Sogo, J.M., Lopes, M. & Foiani, M. Fork reversal and ssDNA accumulation at stalled replication forks owing to checkpoint defects. *Science* **297**, 599-602 (2002).

16. Petermann, E., Orta, M.L., Issaeva, N., Schultz, N. & Helleday, T. Hydroxyurea-stalled replication forks become progressively inactivated and require two different RAD51-mediated pathways for restart and repair. *Mol Cell* **37**, 492-502 (2010).

17. Sirbu, B.M.*, et al.* Analysis of protein dynamics at active, stalled, and collapsed replication forks. *Genes Dev* **25**, 1320-1327 (2011).

18. McGlynn, P. & Lloyd, R.G. Recombinational repair and restart of damaged replication forks. *Nat Rev Mol Cell Biol* **3**, 859-870 (2002).

19. Schlacher, K.*, et al.* Double-strand break repair-independent role for BRCA2 in blocking stalled replication fork degradation by MRE11. *Cell* **145**, 529-542 (2011).

20. Hanada, K.*, et al.* The structure-specific endonuclease Mus81 contributes to replication restart by generating double-strand DNA breaks. *Nat Struct Mol Biol* **14**, 1096-1104 (2007).

21. Doksani, Y., Bermejo, R., Fiorani, S., Haber, J.E. & Foiani, M. Replicon dynamics, dormant origin firing, and terminal fork integrity after double-strand break formation. *Cell* **137**, 247-258 (2009).

22. Wang, Y.*, et al.* Regulation of Set9-mediated H4K20 methylation by a PWWP domain protein. *Mol Cell* **33**, 428-437 (2009).

23. Malovannaya, A.*, et al.* Analysis of the human endogenous coregulator complexome. *Cell* **145**, 787-799 (2011).

24. Matsuoka, S.*, et al.* ATM and ATR substrate analysis reveals extensive protein networks responsive to DNA damage. *Science* **316**, 1160-1166 (2007).

25. Hall-Jackson, C.A., Cross, D.A., Morrice, N. & Smythe, C. ATR is a caffeine-sensitive, DNA-activated protein kinase with a substrate specificity distinct from DNA-PK. *Oncogene* **18**, 6707-6713 (1999).

26. Cotta-Ramusino, C.*, et al.* Exo1 processes stalled replication forks and counteracts fork reversal in checkpoint-defective cells. *Mol Cell* **17**, 153-159 (2005).

27. Branzei, D. & Foiani, M. Maintaining genome stability at the replication fork. *Nat Rev Mol Cell Biol* **11**, 208-219 (2010).

28. Wang, X.*, et al.* Rad17 phosphorylation is required for claspin recruitment and Chk1 activation in response to replication stress. *Mol Cell* **23**, 331-341 (2006).

29. Errico, A. & Costanzo, V. Differences in the DNA replication of unicellular eukaryotes and metazoans: known unknowns. *EMBO Rep* **11**, 270-278 (2010).

30. Lukk, M.*, et al.* A global map of human gene expression. *Nat Biotechnol* **28**, 322-324 (2010).

31. Higgins, N.P., Kato, K. & Strauss, B. A model for replication repair in mammalian cells. *J Mol Biol* **101**, 417-425 (1976).

32. Fujiwara, Y. & Tatsumi, M. Replicative bypass repair of ultraviolet damage to DNA of mammalian cells: caffeine sensitive and caffeine resistant mechanisms. *Mutat Res* **37**, 91-110 (1976).

33. Postow, L.*, et al.* Positive torsional strain causes the formation of a four-way junction at replication forks. *J Biol Chem* **276**, 2790-2796 (2001).

34. Murfuni, I.*, et al.* The WRN and MUS81 proteins limit cell death and genome instability following oncogene activation. *Oncogene* (2012).

Supplementary Information is linked to the online version of the paper at www.nature.com/nature

Acknowledgements We thank P. Russell and J. Karlseder for suggestions and reading of the manuscript. Confocal microscopy was performed at the Waitt Advanced Biophotonics Center. IMV is an American Cancer Society Professor of Molecular Biology, and holds the Irwin and Joan Jacobs Chair in Exemplary Life Science. This work was supported in part by grants from the Department of Defense (W81XWH-10-1-0963), the NIH Cancer Center Core Grant (P30 CA014195-38) Ipsen/Biomeasure, Sanofi Aventis, and the H.N. and Frances C. Berger Foundation. The content is solely the responsibility of the authors and does not necessarily represent the official views of the National Cancer Institute.

Author contributions M.P. designed and performed all experiments, analyzed the data and prepared the manuscript. I.M.V. supervised the work and edited the manuscript.

Author information The authors declare no competing financial interests. Correspondence and requests for materials should be addressed to I.M.V. (verma@salk.edu)

FIGURE LEGENDS

Figure 1 Phosphorylation of ZMYND8 is required for survival after replication stress.

a, Schematic of the ZMYND8 protein showing predicted domains and the position of serine 1060 in an ATM/ATR consensus (SQ) site. **b,** Expression of ZMYND8 was analyzed in different cell lines by western blot with a polyclonal antibody. **c,** Endogenous ZMYND8 was immunoprecipitated from U2OS cells after treatment with different doses of HU for 1 hour. ZMYND8 phosphorylation (pZMYND8) was detected by western blot with an anti-phosphoSQ antibody. **d,** U2OS cells were harvested after the indicated time in 1 mM HU and the phosphorylation of ZMYND8, CHK1 and H2AX determined in immunoprecipitates or lysates as indicated. **e**, Mutation of serine 1060 to alanine (S1060A) blocks the phosphorylation of ZMYND8. HA-tagged ZMYND8 was immunoprecipitated and the phosphorylation after HU determined by western blot. **f,** ZMYND8 phosphorylation after HU (1mM for 1h) is blocked by the ATR inhibitor caffeine (10 mM), but not by the ATM inhibitor KU55933 (10 μM). **g,** Knockdown of ZMYND8. U2OS cells were infected with lentiviral vectors expressing shRNA against ZMYND8 or control (Luciferase). **h, i,** Cells were treated with different doses of HU for 24 hours, and then grown for 8 to 10 days. Colonies were stained with crystal violet and counted. Clonogenic survival is shown as percentage of respective untreated cells. **j,** Clonogenic survival was determined after 24 hour treatment with different doses of aphidicolin. **k,** ZMYND8 phosphorylation is required during HU response. ZMYND8 knockdown cells were reconstituted with sh-resistant wildtype or S1060A-mutant ZMYND8 and HU sensitivity tested in clonogenic survival assays. Survival curves of

knockdown and control cells (from panel i) are shown as grey dashed lines. All data shown are means ± s.d. (n=3 independent experiments). Asterisks indicate significance in two-tailed t-tests (*, $p<0.05$; **, $p<0.01$).

Figure 2 ZMYND8 is required for swift restart of stalled replication forks.

a, ZMYND8 is required for restart after HU-stalling. Replication forks were labeled in U2OS cells with IdU and CldU as indicated in the scheme, DNA fibers spread on glass slides, and tracks detected by immunofluorescent staining. Replication track lengths were measured and are shown as box plots. A Mann-Whitney U-test was performed to compare track lengths (n>100). **b,** Replication fork progression after restart. The graph shows median CldU track lengths at 30 min (from panel a) and 45 min after HU removal. The speed of replication fork progression (the slope of the lines) appears similar between shZMYND8 and control cells. **c,** Percentage of forks that have restarted (showing CldU incorporation) was determined 20 min after HU removal. **d,** ZMYND8 knockdown cells were reconstituted with shRNA-resistant S1060A or wildtype ZMYND8. The phosphorylation site-mutant S1060A does not rescue fork restart after HU.

Figure 3 ZMYND8 localizes near stalled forks and prevents fork reversal.

a, DNA fibers were prepared from U2OS cells after 30 min IdU labeling followed by 1 hour stalling in 3 mM HU. Tracks from ZMYND8 knockdown cells show a strong increase in fluorescence intensity at one end (indicated by arrows). Scale bar, 5 μm. **b,** Quantification of (a). Fluorescence intensity was measured along >100 individual tracks. A significant increase in fluorescence intensity (greater three standard deviations above the mean) was classified as drumstick morphology. **c,** U2OS cells were labeled with CldU and IdU as indicated and then stalled with 3 mM HU for 1 hour. Reverse

orientation or overlay of red and green signal (yellow) demonstrates fork reversal in shZMYND8 cells as illustrated in the schematic. Scale bars, 2 μm. **d,** Cells were pulse-labeled as illustrated for 5 minutes with EdU and fixed directly or after 30 minute thymidine chase, to allow replication forks to move on. The EdU-labeled chromatin was purified by iPOND, and proteins detected in the EdU pull-down and in cell lysates (input) by western blot as indicated. **e,** U2OS cells were labeled with EdU for 8 minutes and then stalled for 1 hour by the addition of 3 mM HU directly to EdU-containing media. After HU addition, replication and EdU incorporation continue until nucleotides are depleted, which leads to more DNA being labeled (increased histone H3 levels in lanes 2 and 4). RAD51 increases at stalled forks in shZMYND8 cells (lane 4).

Figure 4 Fork reversal in ZMYND8 knockdown cells leads to aberrant restart

a, Survival decreases with time of HU treatment. U2OS cells were treated for the indicated times with HU in clonogenic survival assays. Means ± s.d. (n=3) are shown. Asterisks indicate a highly significant difference between shLuciferase and shZMYND8 cells by two-tailed t-test. **b,** Fiber assays were performed after 5 hour HU-stalling as indicated in the scheme. Gaps (indicated by white brackets) between corresponding IdU and CldU tracks indicate fork movement during stalling. **c,** Replication forks in ZMYND8 knockdown cells incorporate nucleotides during stalling. Replication was stalled with 1 mM HU in CldU-containing media for 3 hours as indicated. CldU track lengths were compared by Mann-Whitney U-test. **d,** Cells were labeled with BrdU for 24 h before HU stalling for 5 h. Single-stranded DNA was detected by anti-BrdU staining under non-denaturing conditions. All cells stained BrdU positive under denaturing conditions (+HCl). Scale bars, 10 μm.

Figure 5 Elevated ZMYND8 expression protects cells from replication stress.

a, b, ZMYND8 was overexpressed from a lentiviral vector in U2OS cells (a) and the sensitivity to different HU-doses determined in clonogenic survival assays (b). Means ± s.d. (n=3) are shown. Asterisks indicate highly significant ($p<0.01$) difference in two-tailed t-tests between control and ZMYND8-overexpressing cells. The survival curve of shZMYND8 cells (from Figure 1i) is shown in grey. **c,** Control cells and ZMYND8 overexpressing cells were pulse labeled for 5 minutes with EdU before HU stalling for 3 hours. Overexpression increases the levels of ZMYND8 on the chromatin near replication forks as detected by iPOND. **d,** Model of the role of ZMYND8 at stalled forks. Phosphorylation of ZMYND8 by ATR prevents the reversal of stalled forks, which would lead to RAD51-dependent recombination and genomic instability. In the presence of ZMYND8 forks can be stabilized (by an unknown) mechanism, which allows cells to resume replication after stress.

LEGENDS TO SUPPLEMENTARY FIGURES

Supplementary Figure S1 Expression and localization of ZMYND8.

a, b, ZMYND8 expression in U2OS and HeLa cells was analyzed by western blotting. Low molecular weight bands (asterisks), which are recognized by a monoclonal antibody, are not detected by the polyclonal antiserum (a) and are not affected by knockdown with siRNA (b), and are therefore considered non-specific. **c,** Ectopically expressed full-length ZMYND8 co-migrates with the endogenous protein. **d,** Immunostaining with anti-HA antibody shows exclusively nuclear localization of HA-tagged ZMYND8 in U2OS cells. **e,** Cells were fractionated in cytoplasmic, soluble nuclear (extracted by 200 mM NaCl, 1% NP-40), and chromatin-associated fractions. Equal aliquots were used in western blots and probed for ZMYND8, mTOR, CHK1 and histone H3.

Supplementary Figure S2 Phosphorylation of ZMYND8 after DNA damage

a, HA-tagged ZMYND8 was immunoprecipitated from HeLa cells 1 hour after 10 Gy IR. Levels of ZMYND8 phosphorylation (pZMYND8) were determined by western blotting with an anti-phosphoSQ antibody. Mutation of serine 1060 to alanine blocks the phosphorylation. **b,** ATM is required for ZMYND8 phosphorylation. ATM inhibitor KU55933 (10μM) was added to the media for 1 hour before and after 10 Gy as indicated. ZMYND8 phosphorylation was detected in anti-HA immunoprecipitates. CHK2 Thr68 phosphorylation was detected by western blot in whole cell lysates. **c,** HA-tagged ZMYND8 was immunoprecipitated from U2OS cells at different time points after 10 Gy

and its phosphorylation detected by western blot. **d,** endogenous ZMYND8 was immunoprecipitated from U2OS cells 1 hour after different doses of IR, and the level of phosphorylation determined by western blot. **e, f,** Sensitivity of HeLa (e) and U2OS cells (f) to different doses of IR was determined in clonogenic survival assays after knockdown of ZMYND8, Luciferase (negative control), or BRCA1 (positive control). Means ± s.d. of three independent experiments are shown.

Supplementary Figure S3 Expression of shRNA-resistant ZMYND8.

Wildtype and S1060A-mutant ZMYND8 were made shRNA-resistant through silent point mutations in the shRNA targeting sequence (as described in Materials and Methods). Infection with a lentiviral vector that contains both shRNA and ZMYND8 open reading frame knocks down the endogenous protein and reconstitutes expression to a similar level in U2OS cells.

Supplementary Figure S4 Drumstick morphology of stalled forks in shZMYND8 cells.

a, U2OS cells were sequentially labeled with CldU and IdU before HU-stalling as indicated. The tip of the drumsticks (arrow) in tracks from shZMYND8 cells represents the end of the track that was replicated just before stalling. **b,** Fluorescence intensity was measured along replication tracks (from Figure 3a). Mean ± s.d. of ten tracks are plotted. Fluorescence intensity along tracks from control cells is rather constant. In shZMYND8 cells the fluorescence intensity increases approximately 2-fold at the tip compared to the

rest of the track, consistent with a reversal of the labeled nascent DNA as indicate in the schematic drawing.

Supplementary Figure S5 Aberrant restart of stalled forks in shZMYND8 cells.

a, Fork movement during 1 mM HU. Gaps (marked by white brackets) between IdU and CldU tracks in ZMYND8 knockdown cells (see also Figure 4b) increase in length with HU exposure time. Scale bars are 10 μm. **b,** Cells were stalled in the presence of CldU (as in Figure 4c) to monitor DNA synthesis during stalling as indicated in the schematic. Aphidicolin (1 μg/ml) was added 30 min after HU to block the restart of replicative polymerases.

Supplementary Figure S6 ZMYND8 knockdown cells develop RPA foci during stalling.

U2OS cells were treated with 1 mM HU for the indicated time and stained with antibodies against RPA2 and γH2AX. The number of foci-positive cells was counted (>200 cells) from 3 independent experiments. An increased number of RPA foci positive cells was found in ZMYND8 knockdown cells. Similar percentages of γH2AX-positive cells indicate similar number of cells in S-phase affected by replication stress.

Supplementary Figure S7 Replication checkpoint activation in cells lacking ZMYND8.

Phosphorylation of histone H2AX (γH2AX), CHK1 serine 317 and serine 345 and PCNA levels in U2OS cells were determined by western blotting with respective antibodies after

the indicated time of 1 mM HU treatment. PCNA monoubiqitination leads to a mobility shift (Ub-PCNA), which is only weakly induced by HU and appears similar between ZMYND8 knockdown and control cells .

Supplementary Figure S8 ZMYND8 expression in normal tissues and cancer. ZMYND8 expression was analyzed in a consistently normalized set of data from the gene expression atlas[30]. Log_2 transformed expression levels of ZMYND8 in 1600 samples from cancers and normal tissues (see Methods for details) are shown (means ± s.e.m.). A nested ANOVA was performed to analyze the variance of ZMYND8 expression between normal tissues and cancer.

Figure 1
(Preyer and Verma)

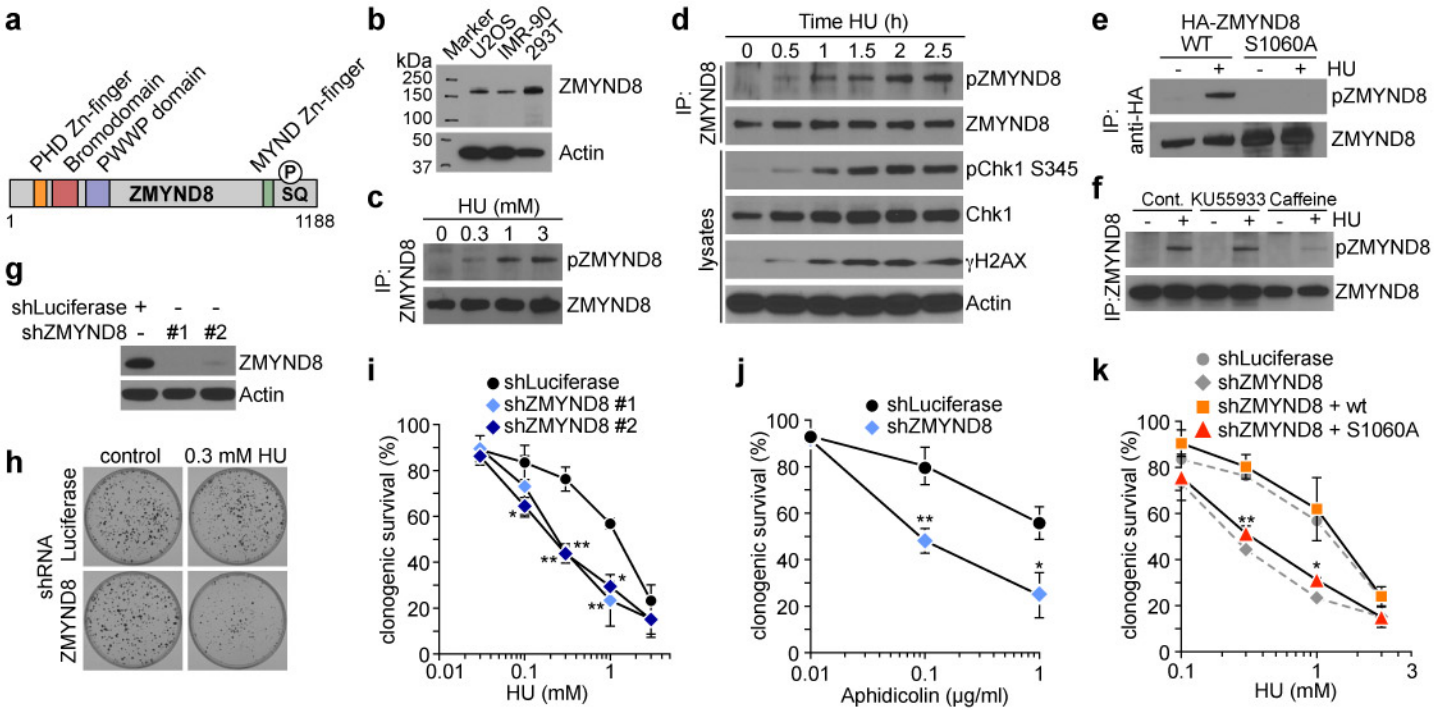

Figure 2
(Preyer and Verma)

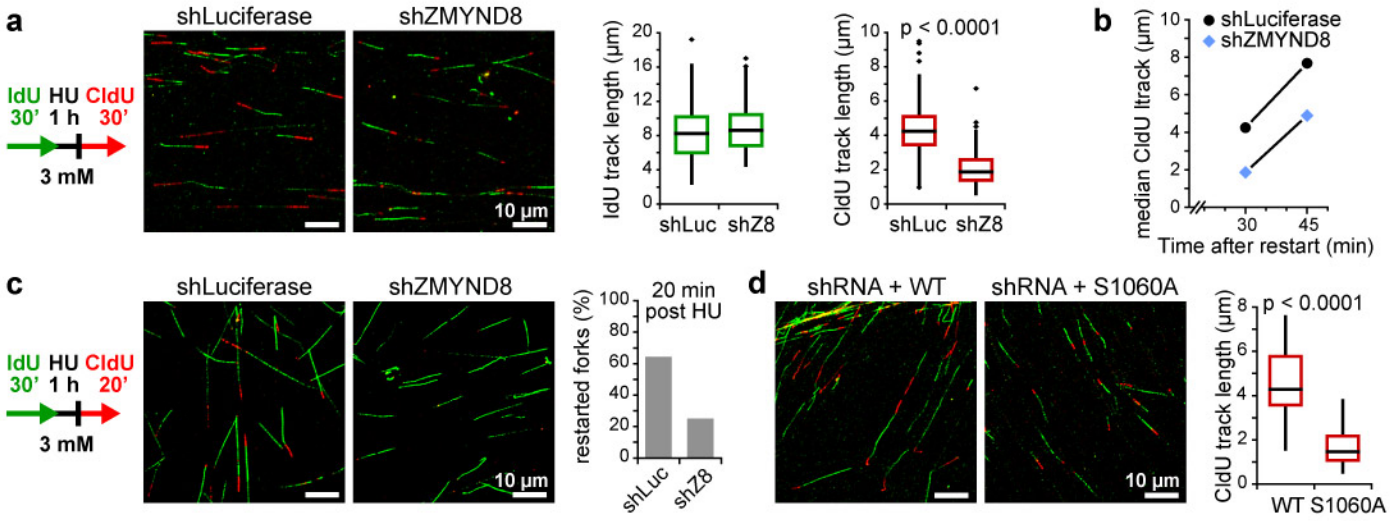

Figure 3
(Preyer and Verma)

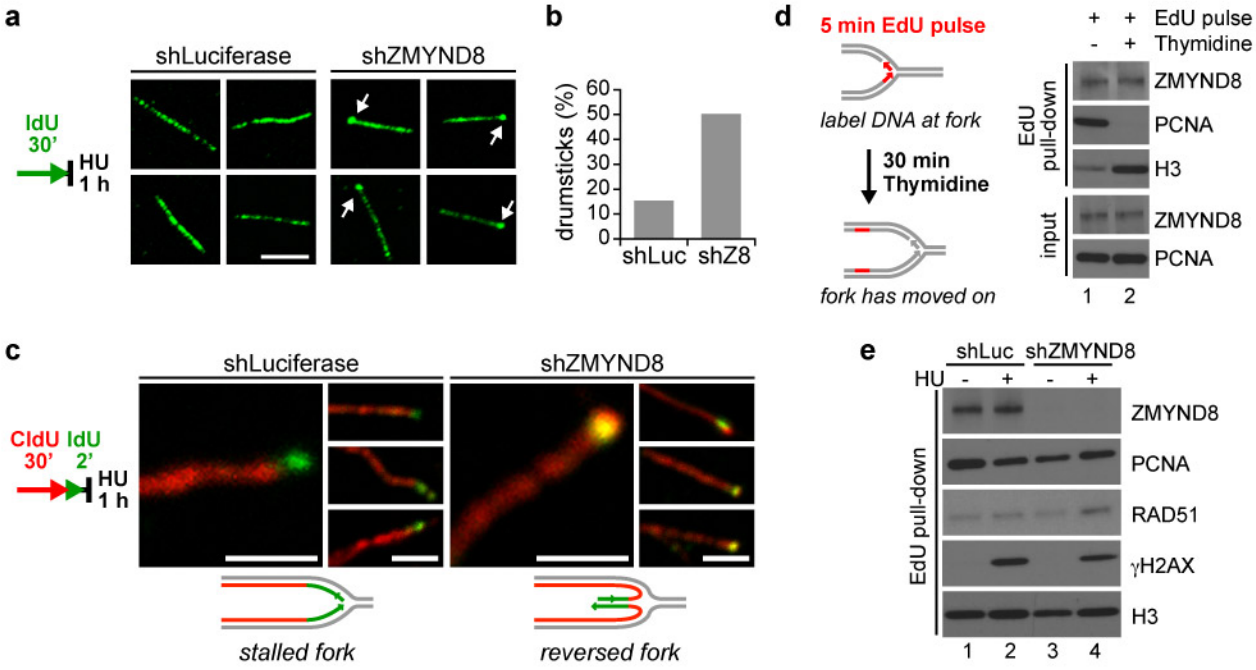

Figure 4
(Preyer and Verma)

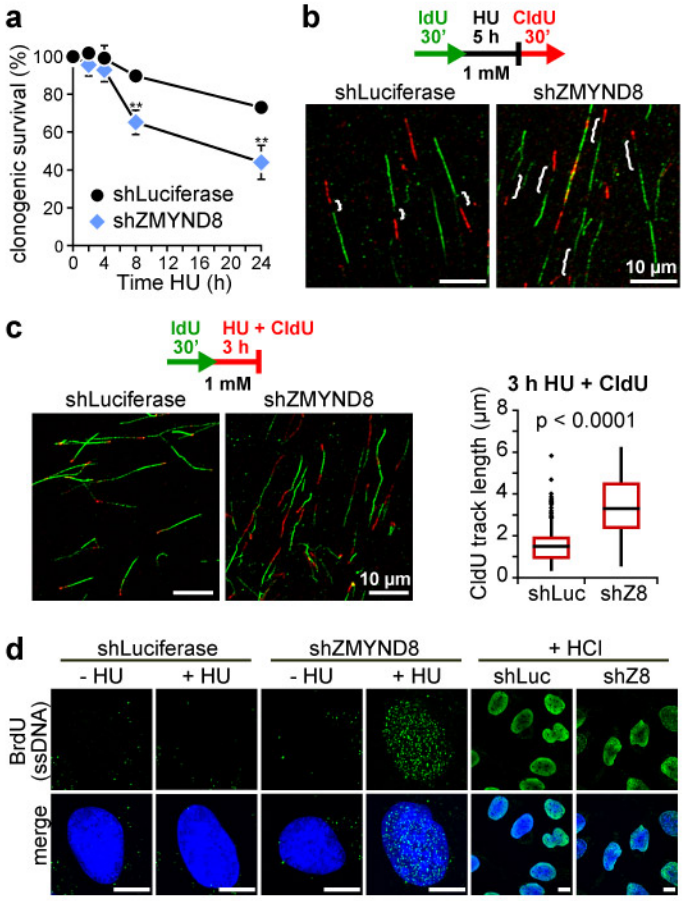

Figure 5
(Preyer and Verma)

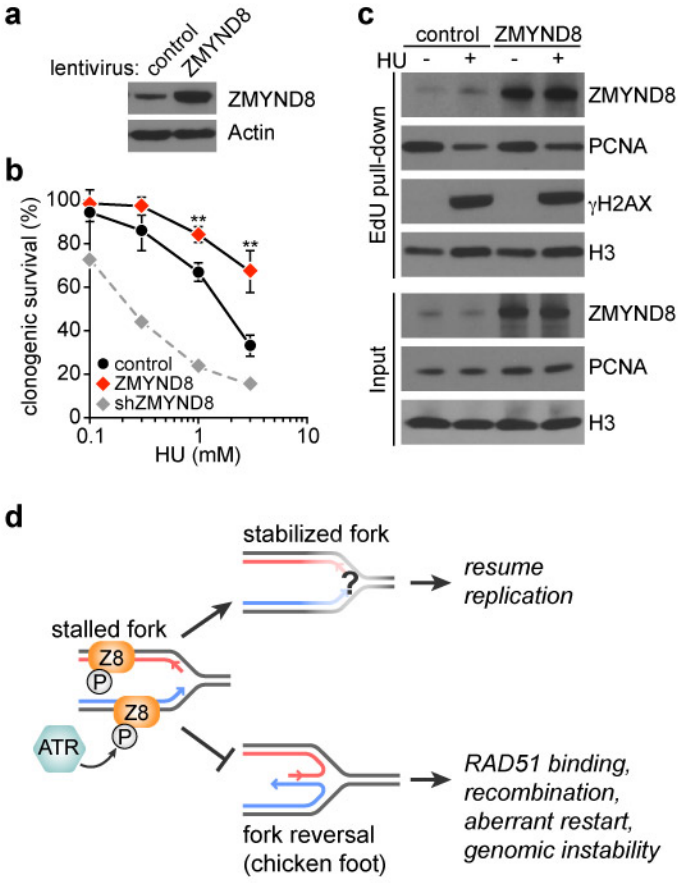

Supplementary Figure S1 (Preyer and Verma)

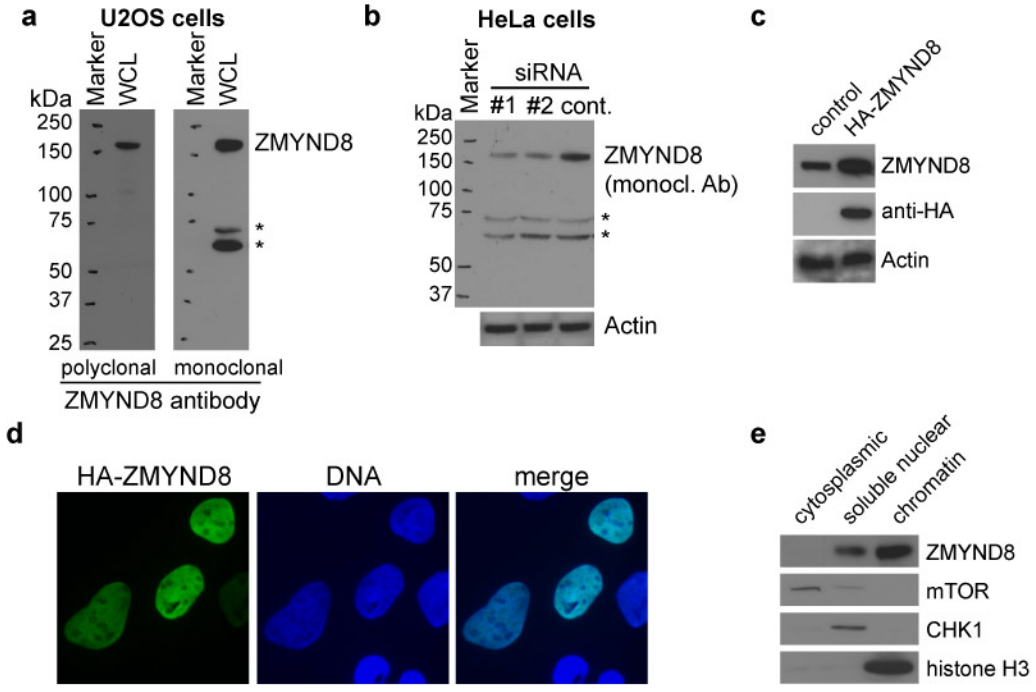

Supplementary Figure S2
(Preyer and Verma)

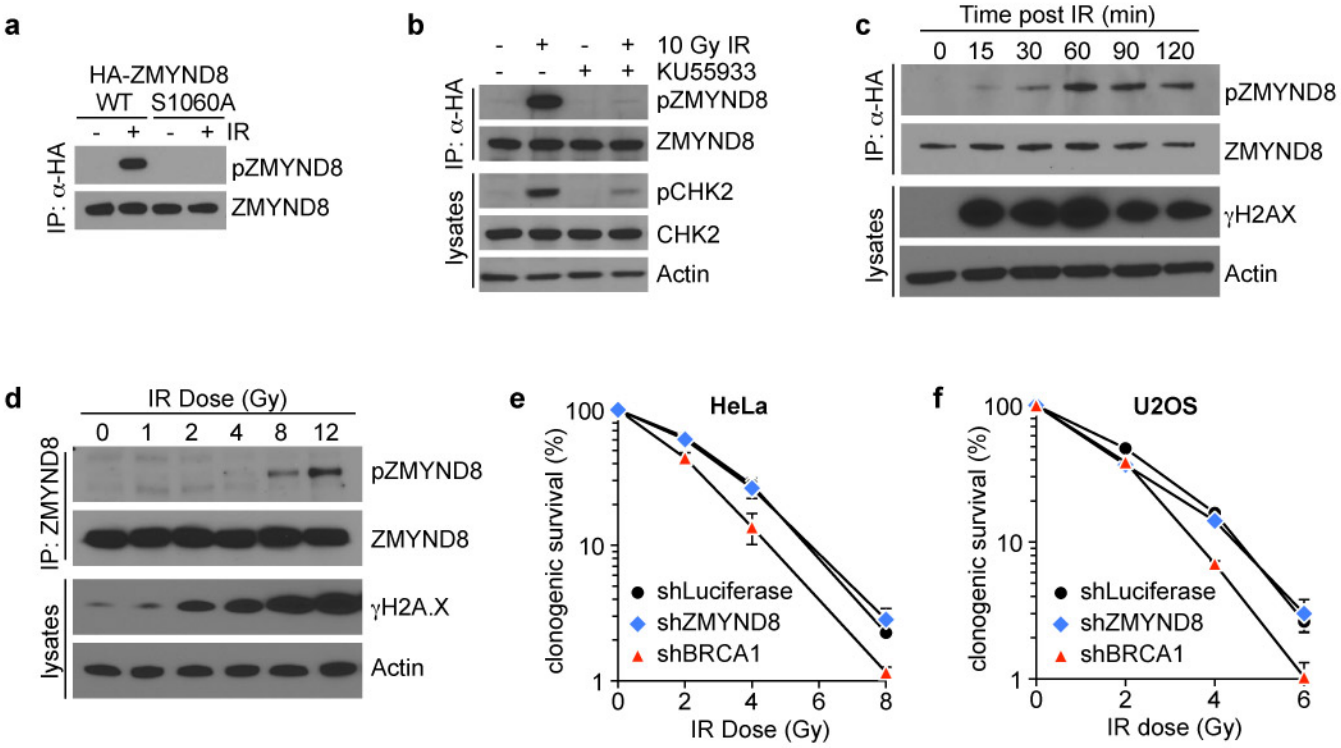

Supplementary Figure S3
(Preyer and Verma)

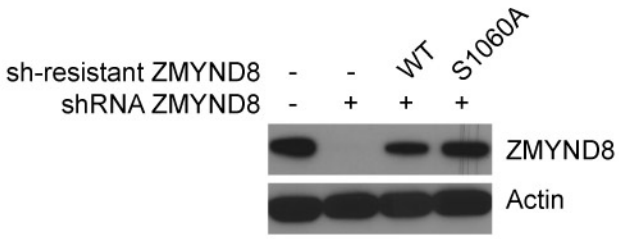

Supplementary Figure S4
(Preyer and Verma)

a

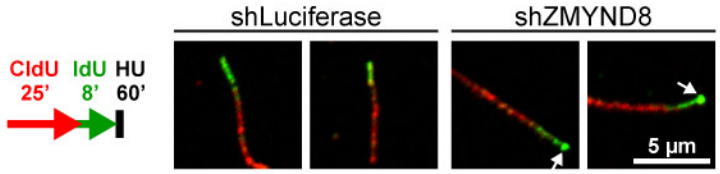

b

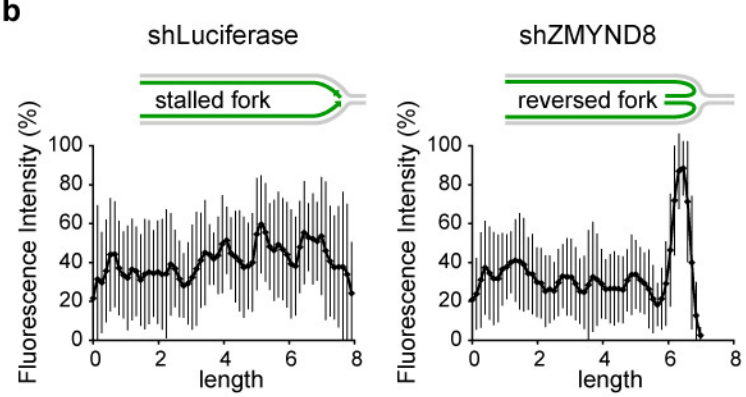

Supplementary Figure S5
(Preyer and Verma)

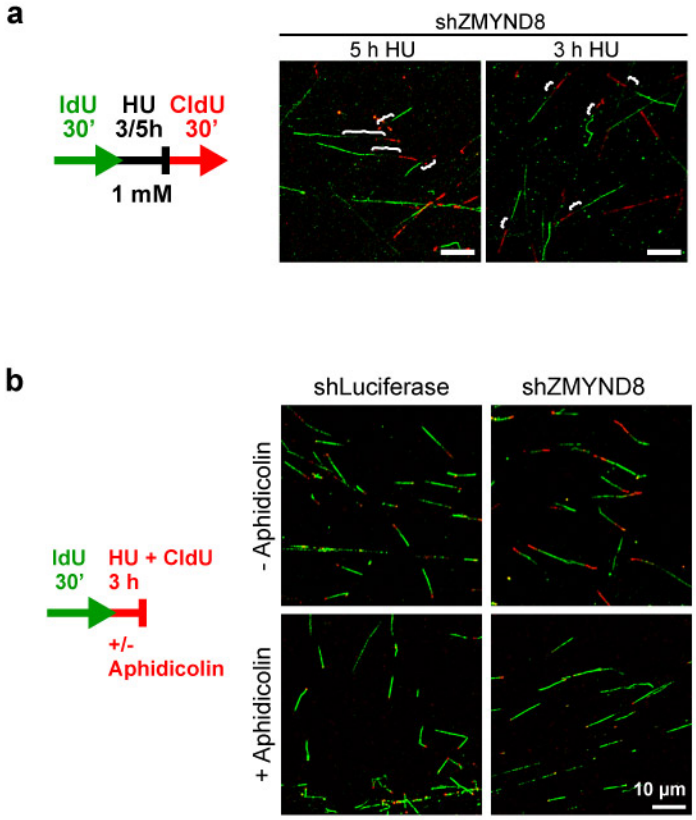

Supplementary Figure S6
(Preyer and Verma)

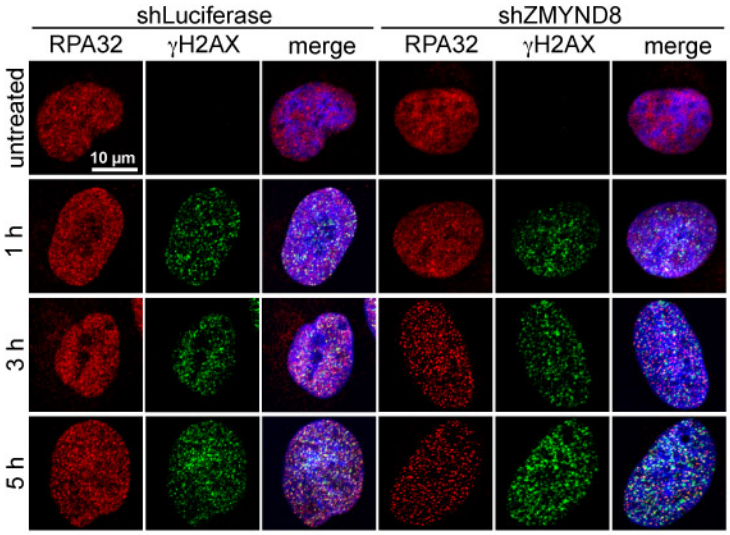

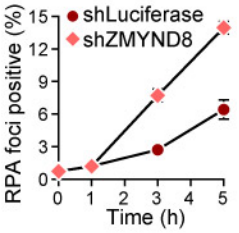

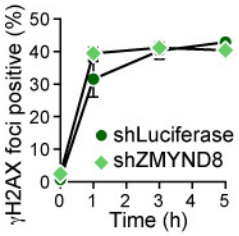

Supplementary Figure S7
(Preyer and Verma)

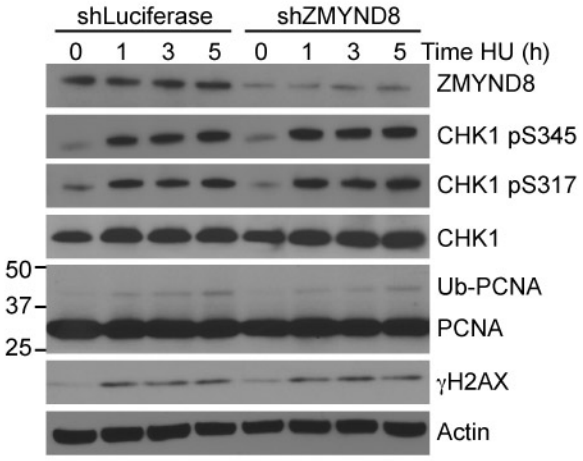

Supplementary Figure S8
(Preyer and Verma)

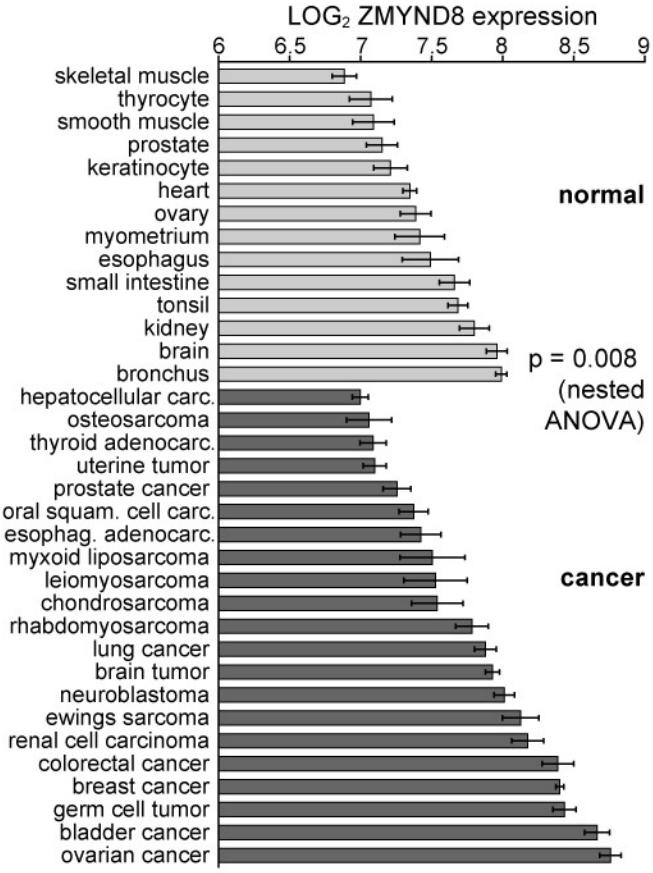

A genetic screen identified RACK7 as a novel factor involved in BRCA1-mediated DNA damage sensitivity pathway

Quan Zhu[1], Gerald M. Pao[1], Dinorah Friedmann-Morvinski[1], Niels Bjarne Woods[1], Summit Chanda[2], Inder M. Verma[1]
[1]Laboratory of Genetics, The Salk Institute for Biological Studies, La Jolla, CA 92037, [2]

Infectious and Inflammatory Disease Center, The Sanford-Burnham Institute

Corresponding author: Inder M Verma: verma@salk.edu

Abstract

BRCA1 is a tumor suppressor whose mutations can account for a large portion of the inherited cases of breast and ovarian cancers. To study the biological function of BRCA1, we performed genetic screening using a lenti-viral vector based cDNA library which expresses 17,500 full-length human and mouse genes. The library features a number of novelties over traditional ones, including broader target cell range, high efficiency, high quality, easier recovery of target genes and full length cDNAs. BRCA1 deficient HCC1937 cells are unusually sensitive to DNA damage induced by gamma irradiation. We exploited this sensitivity to screen for dominant suppressors of this phenotype by introduction of the lentiviral library and have identified a number of candidates that are involved in DNA damage repair pathway mediated by BRCA1, which is an important aspect of tumor suppression of the molecule. One of such factors, ncPKCBP, can specifically cooperate with/substitutes BRCA1 in DNA damage repair pathway in HCC1937 cells. ncPKCBP downregulates the expression levels of a poorly characterized protein, RACK7, which inversely correlates with the function of BRCA1 in DNA damage response. More interestingly, we have identified that the expression levels of RACK7 is elevated in BRCA1 deficient breast cancer cell line and human breast tumor samples. Our data suggested that RACK7 is a novel DNA damage response factor that modulates the DNA-damage-hypersensitivity of BRCA1-deficient breast cancer cells. Moreover, the screening methodology reported here will not only uncover genes involved in BRCA1 tumor suppressor function but also lead to a general application to functional studies in cancer biology.

Introduction

Breast cancer is one of the major causes of oncologic morbidity and mortality in women in the United States. Of these about 5-10% are due to a genetic predisposition to such cancers (American Cancer Society: Overview, breast cancer, Atlanta, GA). BRCA1, as well as BRCA2, were identified as the hereditary breast and ovarian cancer susceptibility

genes that can account for almost all the entirety of inherited cases of breast cancers [1-3]. The penetrance of these mutations is rather high and can confer up to a 85% probability of developing breast cancer by the age of 70 in affected individuals [4]. Despite some recent progress in survival rate, BRCA1-mutated tumors in metastatic patients are extremely difficult to be completely eradicated. Therefore, understanding the biochemical and genetic properties of BRCA1 will lead to the development of more specific and efficient treatment to the patients.

BRCA1 is a large nuclear phosphoprotein that is largely devoid of any recognizable sequence motifs that would readily reveal its function at the molecular level. The recognizable sequence features are a RING finger at the N-terminus of BRCA1 and two copies of the BRCA C-terminal (BRCT) repeat, a motif now found to bind to phospho-peptides in a number of nuclear proteins involved in DNA repair and cell cycle checkpoint proteins [5,6]. The RING finger, which was initially thought to be protein-protein interaction motif, turned out to contain the only known enzymatic function of BRCA1, namely that of an ubiquitin E3 ligase [7-9]. Mouse and human BRCA1 are relatively less conserved at the amino acid sequence level (58%) but functionally human equivalents can rescue the embryonic lethality of BRCA1 mutant mice implying a functional conservation of the protein [10-12].

Over the last decade there has been steady progress in attempts to define the precise molecular roles of BRCA1 in important physiological processes such as transcription, DNA repair, its ubiquitin E3 ligase activity, centrosome function, X-inactivation and heterochromatin, as well as a regulator of cell growth (for reviews see [1,2,12-14]}. It was demonstrated that BRCA1 has a function in transcription in the C-terminus [15,16]. Moreover, introduction of point mutations and small deletions within this domain that occur in BRCA1 cancer patients abrogated this activity completely. Furthermore, BRCA1 binds a number of coactivators such as p300/CBP, RNA Helicase A, and is part of the RNA polymerase II holoenzyme [1,2].

A preponderance of evidence to date implicates BRCA1 in DNA repair and DNA damage in order to preserve chromosome integrity [3,12,13]. BRCA1 was shown to localize to subnuclear foci containing RAD51 during S and G2 phases of cell cycle [17]. RAD51 is an integral component of a type of damage repair known as homologous recombination (HR) which repairs double-strand breaks (DSBs) and interstrand crosslinks [18]. In mitotic cells forced to arrest DNA replication or damaged by UV light, BRCA1 and RAD51 move from their native foci and relocate to sites of DNA synthesis. All these changes occur with concomittent phosphorylation of BRCA1. Mouse embryonic stem cells defective of BRCA1 show a 80-90% reduction in repair of DSB by HR [19]. BRCA1 may also play a role in nucleotide excision repair by transcription coupled repair [20]. Finally BRCA1 has been shown to colocalize with RAD50-MRE11-NBS complex [21] which is thought to be involved in processing of DNA DSBs in both HR and non-homologous end joining (NHEJ) mechanism of repair [22]. It appears that the recruitment of BRCA1 complex to the DNA damage site requires not only its phosphorylation but also ubiquitination of histones mediated by other ubiquitin ligases, RNF8 and RNF163 {Doil, 2009 #3332;Stewart, 2009 #3333;Wu, 2009 #3340}. More recent data revealed a role of BRCA1 in maintaining the integrity of heterochromatin thereby promoting the cellular genomic stability (Zhu et al., 2011).

One in five clinically relevant mutations of BRCA1 occur within the N-terminal 100 residues which contain the RING motif (residues 26-76) documented to have E3 ubiquitin ligase activity [23,24]. It was shown that the RING domain of BRCA1 exhibits E3 ligase activity in vitro [7,8], and all the cancer predisposing mutations in the RING

domain that were tested have inactivated BRCA1 E3 ubiquitin ligase activity[7]. Human BARD1 has been suggested to involve in BRCA1-mediated tumor suppression by directly binding to BRCA1 and enhancing its E3 Ub ligase activity [25,26]. The RING domain has been shown to be essential for BRCA1-mediated tumorigenesis [27] . In another recent paper reported that the RING domain of mouse BRCA1 was not involved in induction of mammary tumors [28]. The RING domain mutant used in this study, however, has not been identified in patients with BRCA1 deficient mammary tumors. It is largely unknown how BRCA1 functions as an E3 ligase in vivo. But the ligase activity is essential for BRCA1 to mono-uniquitylate histone H2A in maintaining the integrity of heterochromatin in vivo (Zhu et al., 2011).

Finally the role of BRCA1 in control of cell proliferation has been enigmatic because loss of BRCA1 (BRCA1-/- mice) inhibits cell proliferation contrary to the expectation that loss of a tumor suppressor would lead to hyperproliferation and not a lack thereof. It is interesting to note that loss of BRCA1 has been associated with the expansion of human breast stem cells [29] whereas partial loss of BRCA1 conferred a growth advantage of human luminal progenitors [30].

HIV based lentiviral vectors have shown great potential as a tool for gene delivery. Lentiviral vectors can transduce a wide variety of dividing and non-dividing cells [31]. More interestingly they can transduce both mouse and human embryonic (ES) cells efficiently and upon differentiation, expression of the transgene can be observed in many different cell types [32] , [33]. Transduced mouse ES cells can be implanted in blastocysts to generate chimeric animals. Two cell stage fertilized mouse eggs can be transduced with lentiviral vectors containing foreign genes and upon transplantation in pseudo pregnant mothers give rise to transgenic pups efficiently. Since the first report, lentiviral vectors have been widely used for expressing small hairpin RNA (shRNA), which upon transduction suppress the expression of target genes [34].

Understanding the biochemical and genetic properties of BRCA1 will lead to the development of more specific and efficient treatment to the patients. To this end, we have performed a genetic screening for factors that can substitute BRCA1 in conferring cells to resistance to DNA damage using a lenti-viral vector based cDNA library. We identified a number of such candidates and identified a novel DNA damage response factor, RACK7, that may modulate the DNA-damage-hypersensitivity of BRCA1-deficient breast cancer cells.

Results

Floxed Lenti Full-length cDNA Library Screen

BRCA1 has been found to be involved in multiple cellular processes. However, it is not clear which of these functions contribute to the tumor suppression property of the molecule and how they contribute. A genetic screening for genes that can rescue the phenotype caused by BRCA1 deficiency will shed light on this fundamental question. We have constructed a lentiviral vector-based floxed full-length cDNA expression library which can be used as the cloning system. The library shows the following advantages over the conventional cloning systems: a) the lentiviral vector-based cloning system broadens the target cell range over the ones that use retroviral vector. Lentiviral vectors infect efficiently primary and quiescent cells. b) the vector stocks can be prepared with high titer. c) very unique sequences have been introduced into the lenti-vector (Fig. 1A) to flank the cDNA open reading frame. These sequences (T3 and T7) can be used for PCR isolation of the cDNA clones. d) A LoxP site has been engineered into the vector. Upon CRE virus application, the entire cDNA expression cassette can be excised so that the biological effects generated by the cDNA expression can be reversed. This feature

allows for elimination of false positive clones and thereby conformation of true positive clones during screening. e) Most importantly, the library contains 17,500 full-length human and mouse cDNA sequences that have been characterized by the Mammalian Gene Collection (MGC) Program Team. Since all the cDNA clones are full length and normalized to the same concentration, this library represents a great improvement over any other traditional ones. It should be more powerful in screening genes of interest.

Generation of a lenti full-length cDNA library

We obtained a cDNA library that contains 17,500 full length human and mouse cDNA sequences that have been characterized by the MGC Program team. To transfer the cDNA clones of the library to our lenti-vector (Fig.1A), we used Gateway Cloning System from Invitrogen. This technology is based on site-specific recombinations mediated by a bacteriophage protein. In the presence of specific sequences named attB and attP, the recombinase generates two products containing attL and attR sites, respectively. Similarly, the recombinase recombines two plasmids harboring attL and attR sites and results in attB and attP sites-containing sequences. Since the expression vector harboring the MGC cDNA clones contains attB site, we introduced the attR Gateway cloning cassette into our lenti-vector so that after sequential BP and LR reactions the final products contain the same attB sequence (Fig. 1A). The reaction is rapid, highly efficient, directional, and keeps the same open reading frame of the expression sequence, all of which satisfy the criteria of constructing a high quality cDNA expression library. To validate that the cloning system can efficiently transfer the library to the target lenti-vector, we performed a pilot experiment with a subgroup of the library consisting of 174 genes. After BP and LR reactions, we prepared DNA from 96 of the clones and ran agarose gels following restriction digestion that can excise the lenti-vector backbone (Fig. 1B).

We found that the inserts have a various size ranging from 500 bp to above 3 kb. We then sequenced the inserts with both flanking sequences: T7 and T3 and referenced them by BLAST. The results showed that 67 clones were unique, 10 clones were seen twice, 6 clones were seen three times, and 2 clones were seen four times. The data implied that there was little bias of particular genes after the transfer of the gene pool to our lenti-vector. Furthermore, as the sequencing was performed in both directions flanking the gene we could confirm that in the majority of clones there was no aberrant recombination that would affect gene expression or function. When using the 174 clones to transduce hematopoietic progenitors which were then allowed to develop into colonies originating from a single cell, we achieved a normal transduction efficiency of about 25%, which means the virus is apparently normal. Furthermore, 10 of the 15 bands that we sequenced from PCR amplified inserts of the library from the colonies (where the colonies that underwent no selection) revealed that the 10 sequences were unique as determined by BLAST search.

We next performed BP reaction with 300 ng of the 17,500 cDNA which resulted in a complexity of 2.5×10^6 of the library. 3×10^5 bacterial colonies were harvested after BP reaction, and 300 µg of DNA was obtained. After LR reaction, 3×10^5 bacterial colonies were harvested and yielded 3.3 mg of DNA. This DNA has then been used to generate lentiviral vectors by four plasmid cotransfection into 293T cells. The typical vector titers of the supernatants generated in such manner yield a titer of 10^6 to 10^7 transducing units/ml. This is at least over a 50 fold coverage of the 17,500 initial clones and thus likely to be a good representation of the diversity of the original clones.

Identification and cloning of gene(s) cooperating with BRCA1 to confer resistance

to DNA damage

BRCA1 gene confers resistance to γ-irradiation and DNA damaging agents. We set out to identify other gene(s) that may cooperate, mediate, substitute or serve as substrates for BRCA1. We used a human breast cancer cell line, HCC1937, which is deficient for functional BRCA1. HCC1937 cells are unusually sensitive to DNA damage induced by gamma irradiation. We exploited this sensitivity to screen for dominant suppressors of this phenotype by introduction of the lentiviral cDNA library as described above.

In our experience we typically irradiate 10,000 to 50,000 HCC1937 cells with a dose of 4.5 Gray. At this dose the cells do not survive or form not more than 2 or 3 colonies as an upper limit. BRCA1 reconstituted cells typically form around 20 to 40 colonies under these identical conditions. This indicates that even a full reversal of the BRCA1 defect only leads to approximately to the survival of one out of a 1,000 reconstituted cells. When using a library only single or a few cells are expected to be transduced with any given cDNA, thus irradiation under the same conditions would most likely miss a gene that might rescue or ameliorate the phenotype. Thus we designed a screen based on many rounds of enrichment of lower sublethal doses of radiation that should give selective growth advantage to those genes that had a positive effect on proliferation in the presence of DNA damage. To accomplish this we irradiated HCC1937 cells with incremental doses ranging from 1.0 Gray to 3.0 Gray allowing 48 hrs for recovery (Fig. 2A). We then performed seven rounds of such irradiations. After the final round of irradiation we pooled all the surviving cells and extract DNA from the pooled population. We identified the positive clones by PCR amplification using T3 and T7 primers which flank the cDNA insert. HCC1937 cells that were infected with the library backbone vector were used as controls (Fig. 2B).

As shown in table 1, we cloned a number of candidates. To validate the clones, we cloned candidates 5-1 (Noc-4), 5-5 (PKCBP) and 5-6 (H3.3) into an expression lentiviral vector, pBOB-CAG, and individually transduced them into HCC1937 cells, the cell line used in the initial screening. The infected cells were seeded into T25 flasks in three different cell densities, irradiated with 4.5 Gy, a dosage at which the BRCA1 deficient HCC1937 cells typically do not survive or form not more than 2 or 3 colonies as an upper limit, and kept in culture for at least 30 days before colonies were stained and counted (irradiated cultures). In parallel, 1/10 cells of each culture were seeded into T25 flasks and kept in culture for the same length of time without irradiation (nonirradiated cultures).

To determine the relative irradiation (IR) resistance (relative cell survival), the ratios of colony numbers per flask of irradiated cells to colony numbers of nonirradiated cells were calculated (pairwise) for individual cultures in each experiment. As shown in Fig. 3A, both PKCBP and Noc-4 clones provided IR resistance to HCC1937 cells. The same experiment was repeated three times. For this report, we focused on the role of PKCBP in BRCA1 mediated DNA damage pathway. We transduced HCC1937 cells with both genes (BRCA1 and PKCBP) to test whether these proteins have synergistic or antagonistic effects on irradiation hypersensitivity. The combination of BRCA1 plus PKCBP did not increase IR resistance of HCC1937 cells but lowered the ratio to the levels of PKCBP alone (Fig. 3B).

PKCBP, also known as receptors for activated C-kinase (RACK), is a family of proteins that anchors activated protein kinase C (PKC) isoenzymes and increases both its phosphorylation and the duration of its activation (4). BLAST results from our sequenced PKCBP clone showed high homology with RACK7 protein. RACK7 appears to be expressed in most tissues and is predicted to have two types of zinc fingers (PHD-type

and Mynd-type), a bromo domain that could facilitate binding to acetyl-lysine, as well as a PWWP domain, the function of which is still unclear. The biological function of the Rack7 protein is largely unknown. But surprisingly the clone does not represent the full length protein. The clone consists of 428 bp that localized to the 3' UTR of RACK7 mRNA (we named it ncPKCBP) as shown in the diagram Fig. 3C. From these 428 bp only 105 bp are 100% homologous between human and mouse PKCBP1.
Because one of the important functions of the 3' UTR is to regulate the expression levels of the corresponding mRNA, we next tested the levels of RACK7 mRNA by real-time RT-PCR. Fig. 4A shows the mRNA levels of RACK7 in HCC1937 cells transduced with either BRCA1 or ncPKCBP. Both genes seemed to downregulate the levels of RACK7 mRNA to a similar level. The levels of RACK7 mRNA remained at low level also after irradiation in the resistant HCC1937 colonies reconstituted with BRCA1 (Fig. 4B). Therefore, we have identified a novel factor that regulates the mRNA levels of RACK7 in the absence of BRCA1 indicating an unidentified function of BRCA1 in normal cells.

Differential expression levels of RACK7 in BRCA1-mutated human breast cancer
To access whether the function of ncPKCBP is specific to HCC1937 cells, we next transduced ncPKCBP into another cancer cell line, LAPC4 (Los Angeles Prostate cancer-4) (Fig. 5A). This cell line is also sensitive to irradiation (4.5 Gy) but it has WT p53 and no alterations in BRCA1 protein expression. However, the levels of RACK7 mRNA were not affected when ncPKCBP was overexpressed. Similar results were obtained when HeLa cells were transduced with ncPKCBP (data not shown), suggesting that the novel factor ncPKCBP functions specifically in BRCA1 mediated DNA damage response pathway. We also compared the levels of RACK7 mRNA in these three different cell lines: HCC1937, HeLa and LAPC4 and found that HCC1937 has the highest levels of the three (Fig. 5B). We next analyzed the expression levels of RACK7 in human BRCA1-mutated breast tumors from 5 individual patients. All five tumor samples expressed over 3 fold higher expression of RACK7 than the normal primary human mammary epithelial cells (HMEC). One tumor (B1T1) exhibited 45 fold increased expression of RACK7 mRNA (Fig. 5C) .
Taken together, we have found that absence of BRCA1 and its function in DNA damage response pathway might lead to accumulated levels of RACK7 mRNA in HCC1937 cells since reconstitution of wildtype BRCA1 or a newly identified factor ncPKCBP could diminish the elevation. Therefore, the expression of RACK7 may be an important component in BRCA1 mediated DNA damage pathway and tumor suppression.

Discussion

To study the biological function of the tumor suppressor BRCA1, we have performed genetic screening using a lenti-viral vector based cDNA library which expresses 17,500 full length human and mouse genes. The library features a number of novelties over traditional ones, including broader target cell range, high efficiency, high quality, easier recovery of target genes and full length cDNAs. This methodology will not only uncover genes involved in BRCA1 tumor suppressor function but also lead to a general application to functional studies in cancer biology. We have successfully isolated a

number of candidate genes that may cooperate with BRCA1 to confer resistance to DNA damage (Table 1). We also have further validated our screening and focused on the most promising factor, RACK7 for mechanistic study. We have found that the expression levels of RACK7 is elevated in BRCA1 deficient breast cancer cell line as well as a subset of BRCA1-mutant patient samples (Fig. 5). It was reported that RACK7 is phosphorylated in response to ionizing radiation in a proteomics approach that aimed to characterize targets of the ATM and ATR kinases [35]. This data suggested that RACK7 is a novel DNA damage response factor that modulates the DNA-damage-hypersensitivity of BRCA1-deficient breast cancer cells. In agreement with our data, RACK7 locus has been described as amplified in several breast cancer cells and in familial breast cancer of the luminal subtype. RACK7 over-expression has been correlated to both breast and ovarian cancers. Thus, RACK7 has many features of being a novel breast/ovarian cancer gene. Our working model is that **RACK7 is a novel factor involved in DNA damage response pathway and its function may specifically involve in BRCA1 mutation mediated breast cancer progression**. Moreover, RACK7 could potentially be a novel biomarker indicating the status of radiation and/or chemotherapy resistance of the BRCA1-deficient tumor, thereby providing valuable information for optimal and curative treatment of the BRCA1 mutation carriers.

Materials and Methods

Cell culture and virus infection. Primary neural progenitor cells were isolated from adult mice containing one BRCA1 null allele and one floxed BRCA1 allele as described [36]. The cells were cultured in DMEM/F12 (1:1) medium with N2 supplement (Invitrogen, Carlsbad, CA), 20 ng/ml of human fibroblast growth factor 2 (Peprotech, Rocky Hill, NJ), and 20 ng/ml human epithelial growth factor (Peprotech, Rocky Hill, NJ). Embryonic neural progenitors were isolated and cultured as described [37]. Cultured cells were infected with retrovirus by a 12-h incubation with an MOI of 5 and harvested at the time indicated in corresponding figure legends. To study cell proliferation, 10 μM of BrdU (Sigma-Aldrich, St. Louis, MO) or EdU (Invitrogen, Calsbad, CA) was pulsed for 2 h before fixation. HCC1937 cells were cultured as described [7]. Reconstitution experiments were performed on passage 2 embryonic neural progenitor cells and infected with either retrovirus expressing CRE-GFP or GFP alone. Lentiviral human BRCA1 expressed under the control of CAG promoter or the control GFP was coinfected with the retroviral constructs. Approximately 72 h post infection, cells were harvested with TRIZOL for RNA extraction. Fibroblasts were isolated from P7 mouse ribcages by digestion with 2 mg/ml of pronase (Roche Biochem) for 30 min at 37 °C followed by a 90 min digestion with 3 mg/ml of CollagenaseD (Roche Biochem) in DMEM. Cells were cultured in DMEM 15% FCS with antibiotic/antimycotic and infected with retrovirus as with neural progenitor cells. Cells were left at confluency for 1 week before RNA extraction by TRIZOL.

Quantitative RT-PCR. Reverse transcription was carried out using SuperScript III First-strand Synthesis System (Invitrogen)**.** The quantitation of PCR products was analyzed with SYBR Green using ABI PRISM 7700 Sequence Detection system software (Applied Biosystems).

Acknowledgments

We thank Nina Tonnu, Nien Hoogn for technical support in preparation of lentiviruses.

References

1. Scully R, Puget N (2002) BRCA1 and BRCA2 in hereditary breast cancer. Biochimie 84: 95-102.

2. Scully R, Livingston DM (2000) In search of the tumour-suppressor functions of BRCA1 and BRCA2. Nature 408: 429-432.

3. Tutt A, Ashworth A (2002) The relationship between the roles of BRCA1 genes in DNA repair and cancer predisposition. Trends in Molec Med 8: 571-576.

4. Rahman N, Stratton MR (1998) The genetics of breast cancer susceptibility. Annu Rev Genet 32: 95-121.

5. Yu X, Chini CC, He M, Mer G, J. C (2003) The BRCT domain is a phospho-protein binding domain. Science 302: 639-642.

6. Manke IA, Lowery DM, Nguyen A, Yaffe MB (2003) BRCT repeats as phosphopeptide-biding modules involved in protein targeting. Science 302: 636-639.

7. Ruffner H, Joazeiro CAP, Hemmati D, Hunter T, Verma IM (2001) Cancer-predisposing mutations within the RING domain of BRCA1: Loss of ubiquitin protein ligase activity and protection from radiation hypersensitivity. Proc Natl Acad Sci (USA) 98: 5134-5139.

8. Lorick KL, Jensen JP, Fang S, Ong AM, Hatakeyama S, et al. (1999) RING fingers mediate ubiquitin-conjugating enzyme (E2)-dependent ubiquitination. Proc Natl Acad Sci (USA) 96: 11364-11369.

9. Xia Y, Pao GM, Chen HW, Verma IM, Hunter T (2003) Enhancement of BRCA1 E3 ubiquitin ligase activity through direct interaction with the BARD1 protein. J Biol Chem 278: 5255-5263.

10. Chandler J, Hohenstein P, Swing D, Tessarollo L, Sharan SK (2001) Human BRCA1 gene rescues the embryonic lethality of Brca1 mutant mice. Genesis 29: 72-77.

11. Lane T, Lin C, Brown M, Solomon E, P L (2000) Gene replacement with the human BRCA1 locus: tissue specific expression and rescue of embryonic lethality in mice. Oncogene 19: 4085-4090.

12. Jasin M (2002) Homologous repair of DNA damage and tumorigenesis: the BRCA connection. Oncogene 21: 8981-8993.

13. Venkitaraman AR (2002) Cancer susceptibility and the functions of BRCA1 and BRCA2. Cell 108: 171-182.

14. El-Deiry WS (2002) Transactivation of repair genes by BRCA1. Cancer Biol & Ther 1: 490-491.

15. Chapman MS, Verma IM (1996) Transcriptional activation by BRCA1. Nature 382: 678-679.

16. Monteiro AN, August A, Hanafusa H (1996) Evidence for a transcriptional activation function of BRCA1 C-terminal region. Proc Natl Acad Sci (USA) 92: 13595-13599.

17. Scully R, Chen J, Plug A, Xiao Y, Weaver D, et al. (1997) Association of BRCA1 with Rad51 in mitotic and meiotic cells. Cell 88: 265-275.

18. Baumann P, West SC (1998) Role of the human Rad51 protein in homologous recombination and double-stranded-break repair. Trends in Biochem Sci 23: 247-251.

19. Moynahan M, Chiu J, Koller B, Jasin M (1999) BRCA1 controls homology-directed DNA repair. Mol Cell 4: 511-518.

20. Gowen LC, Avrutskaya AV, Latour AM, Koller BH, Leadon SA (1998) BRCA1 required for transcription-coupled repair of oxidative DNA damage. Science 281: 1009-1012.

21. Zhong Q, Chen C, Li S, Chen Y, Wang C, et al. (1999) Association of BRCA1 with the hRad50-hMre11-p95 complex and the DNA damage response. Science 285: 747-750.

22. Karran P (2000) DNA double strand break repair in mammalian cells. Curr Opin Genet Dev 10: 144-150.

23. Freemont PS (2000) RING for destruction? Curr Biol 10: R84-R87.

24. Joazeiro CA, Weissman AM (2000) RING finger proteins: mediators of ubiquitin ligase activity. Cell 102: 549-552.

25. Hashizume R, Fukuda M, Maeda I, Nishikawa H, Oyake D, et al. (2001) The RING heterodimer BRCA1-BARD1 is a ubiquitin ligase inactivated by a breast cancer-derived mutation. J Biol Chem 276: 14537-14540.

26. Chen A, Kleiman F, Manley J, Ouchi T, Pan Z (2002) Autoubiquitination of the BRCA1*BARD1 RING ubiquitin ligase. J Biol Chem 277: 22085-22092.

27. Drost R, Bouwman P, Rottenberg S, Boon U, Schut E, et al. (2011) BRCA1 RING Function Is Essential for Tumor Suppression but Dispensable for Therapy Resistance. Cancer Cell 20: 797-809.

28. Shakya R, Reid LJ, Reczek CR, Cole F, Egli D, et al. (2011) BRCA1 tumor suppression depends on BRCT phosphoprotein binding, but not its E3 ligase activity. Science 334: 525-528.

29. Liu S, Ginestier C, Charafe-Jauffret E, Foco H, Kleer CG, et al. (2008) BRCA1 regulates human mammary stem/progenitor cell fate. Proc Natl Acad Sci U S A 105: 1680-1685.

30. Lim E, Vaillant F, Wu D, Forrest NC, Pal B, et al. (2009) Aberrant luminal progenitors as the candidate target population for basal tumor development in BRCA1 mutation carriers. Nat Med 15: 907-913.

31. Somia N, Verma IM (2000) Gene therapy: trials and tribulations. Nat Rev Genet 1: 91-99.

32. Lois C, Hong EJ, Pease S, Brown EJ, Baltimore D (2002) Germline transmission and tissue-specific expression of transgenes delivered by lentiviral vectors. Science 295: 868-872.

33. Pfeifer A, Ikawa M, Dayn Y, Verma IM (2002) Transgenesis by lentiviral vectors: lack of gene silencing in mammalian embryonic stem cells and preimplantation embryos. Proc Natl Acad Sci (USA) 99: 2140-2145.

34. Tiscornia G, Singer O, Ikawa M, Verma IM (2003) A general method for gene knockdown in mice by using lentiviral vectors expressing small interfering RNA. Proc Natl Acad Sci (USA) 100: 1844-1848.

35. Matsuoka S, Ballif BA, Smogorzewska A, McDonald ER, 3rd, Hurov KE, et al. (2007) ATM and ATR substrate analysis reveals extensive protein networks responsive to DNA damage. Science 316: 1160-1166.

36. Palmer TD, Markakis EA, Willhoite AR, Safar F, Gage FH (1999) Fibroblast growth factor-2 activates a latent neurogenic program in neural stem cells from diverse regions of the adult CNS. J Neurosci 19: 8487-8497.

37. Nakashima K, Yanagisawa M, Arakawa H, Kimura N, Hisatsune T, et al. (1999) Synergistic signaling in fetal brain by STAT3-Smad1 complex bridged by p300. Science 284: 479-482.

Figure Legends

Fig. 1.Construction of a cDNA lenti-viral library. A. Diagram of the lenti-vector used in the full-length cDNA library. See details in the text. **B.** Validation of the transfer of the cDNA library to the target lenti-vector. Restriction digestion of 96 clones from the subgroup of the full length cDNA library. There is a variety of inserts. 10 clones did not have the correct lenti-backbone. Arrows: the position of the lenti-vector backbone. Asterisks: a positive control for the restriction digestion.

Fig. 2. Library screening and cloning of the gene(s) involved in BRCA-1 mediated DNA damage hypersensitivity. A. A diagram of the library screening procedure. **B**. Isolation of the gene candidates that confer the resistance to DNA damage hypersensitivity in HCC1937 cells.

Fig 3. Effect of BRCA1, Noc-4, PKCBP and H3.3 on protection from irradiation hypersensitivity. **A**. . A diagram of the library screening validation procedure. **B.** HCC1937 cells are infected with lentivirus expressing each of the clones, PKCBP, H3.3, NOC-4,or BRCA1 or GFP as controls prior to be irradiated at 4.5 Gy. The relative IR resistance (relative cell survival) was determined one month after the treatment. **C**. PKCBP expression reduced the IR hypersensitivity of HCC1937 cells. HCC1937 cells are infected with lentivirus expressing PKCBP alone, or BRCA1 alone or coinfected with both viruses prior to be irradiated at 4.5 Gy. The relative IR resistance (relative cell survival) was determined one month after the treatment. **D.** The diagram of the RACK-7 locus and position of clone ncPKCBP.

Fig 4. Analysis of RACK7 mRNA levels by quantitative RT-PCR. A. HCC1937 cells are infected with lentiviruses expressing BRCA1 alone, ncPKCBP alone, Noc-4 alone, or coinfect with BRCA1 and ncPKCBP. **B**. HCC1937 cells reconstituted with a wildtype BRCA1 are irradiated at 4.5 Gy. The survival colonies are subjected to analysis. Total RNA is extracted from each of the cell lines using Tri-sol solution prior to reverse transcription and quantitative PCR to determine the amount of RACK7 mRNA. 18S is used as a normalizer.

Fig 5. Analysis of RACK7 mRNA in different cancer cells by quantitative RT-PCR. Total RNA is extracted from: **A**. LAPC4 cells infected with lentiviruses expressing ncPKCBP or Noc-4 or mock. **B**. HCC1937 cells, Hela cells or LAPC4 cells. C. Human BRCA1-mutant breast tumors prior to reverse transcription and quantitative PCR to determine the levels of RACK7 mRNA. 18S is used as a normalizer.

Table 1. Summary of clones identified after gamma irradiation selection

clone	identity	Accession #	description
5-1	Unknown protein	BC009103	Novel ORF overlapping COX4
5-2	Tumor suppressor	AF156165	Putative tumor suppressor in -5q syndrome
5-4	L36A-like protein	NM_001001	Similar to human Ribosomal protein L36
5-5	ncPKCBP1	BC060508	Protein Kinase C binding protein 1
5-6	H3.3B	BC067757	Histone variant H3.3 B

A

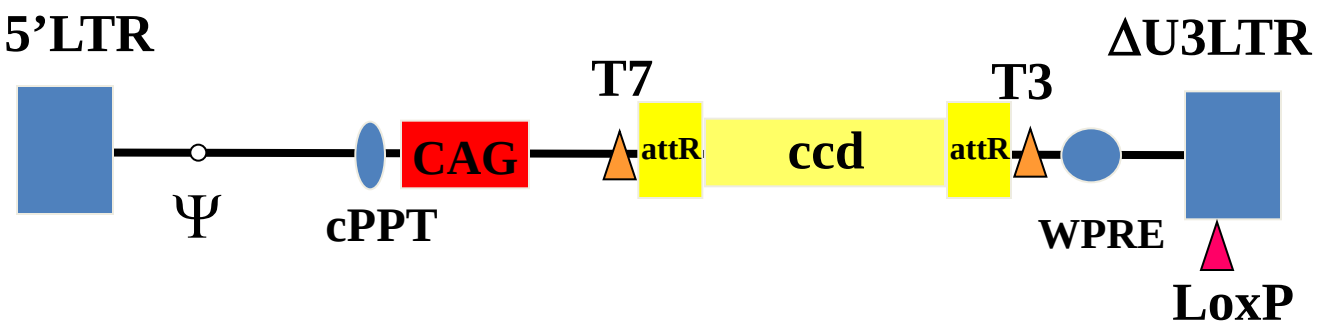
5'LTR
Ψ
cPPT
CAG
T7
attR
ccd
attR
T3
WPRE
ΔU3LTR
LoxP

B

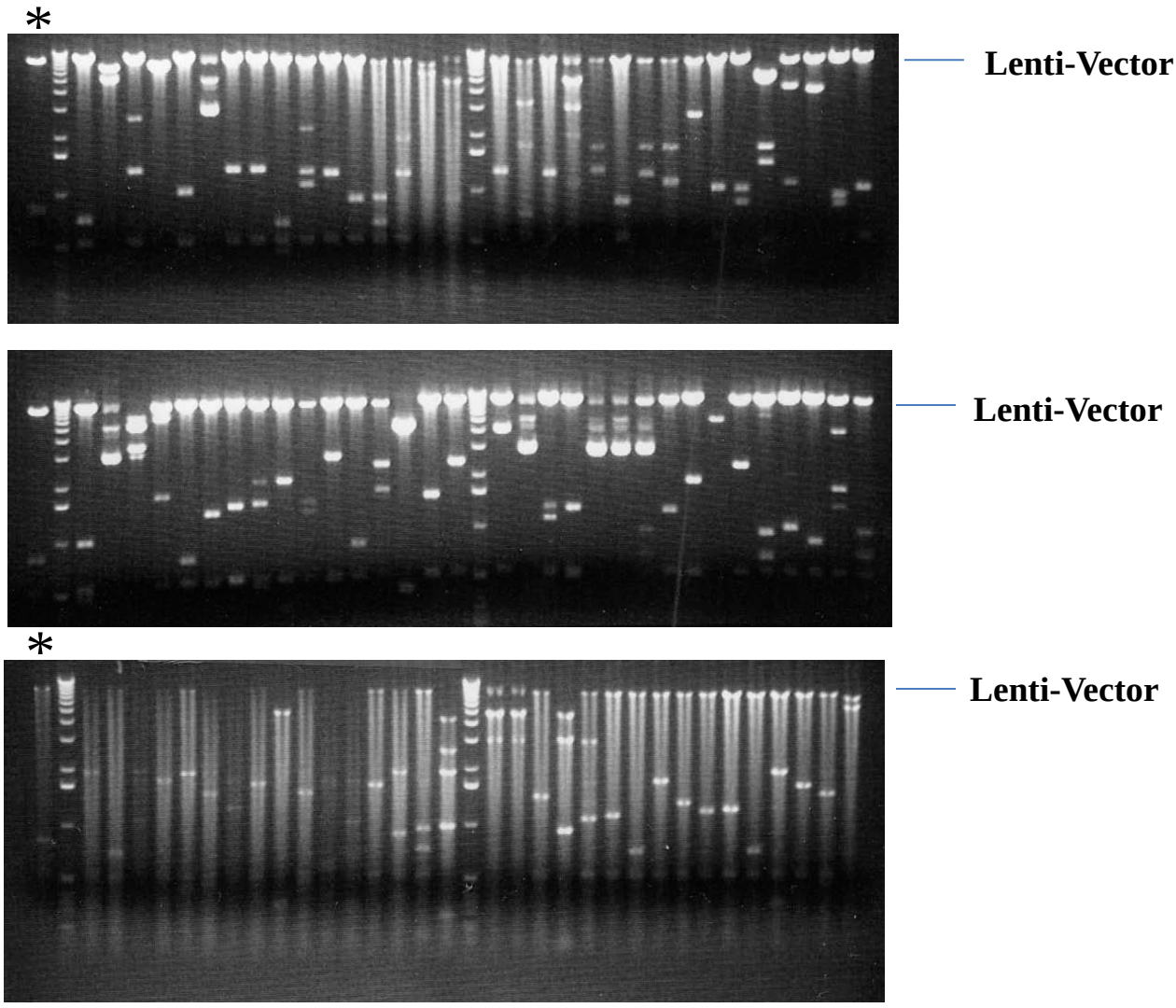
*
Lenti-Vector
Lenti-Vector
*
Lenti-Vector

A

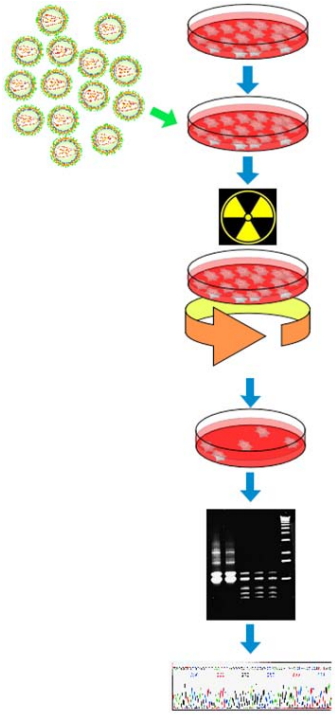

1. HCC1937 cell culture
2. Lentiviral library infection
3. 7 rounds of IR
4. Proliferation of survival clones
5. DNA extraction and PCR
6. Sequencing

B

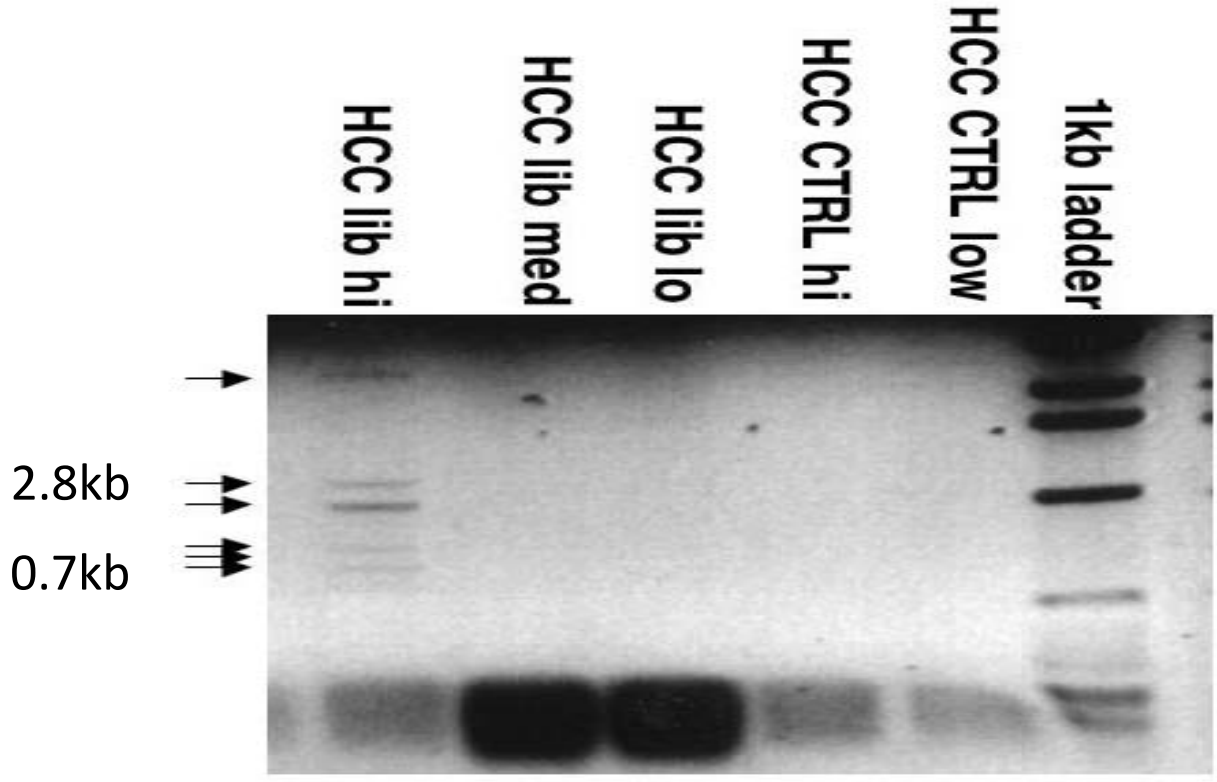

Zhu et al., Fig. 3

A

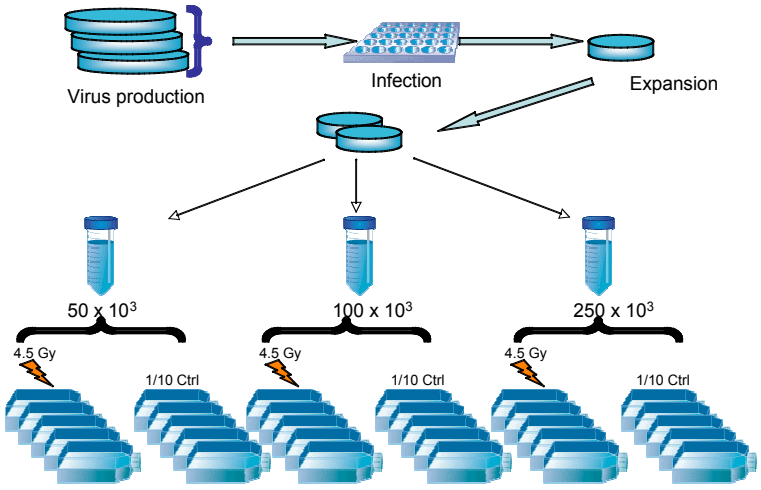

B

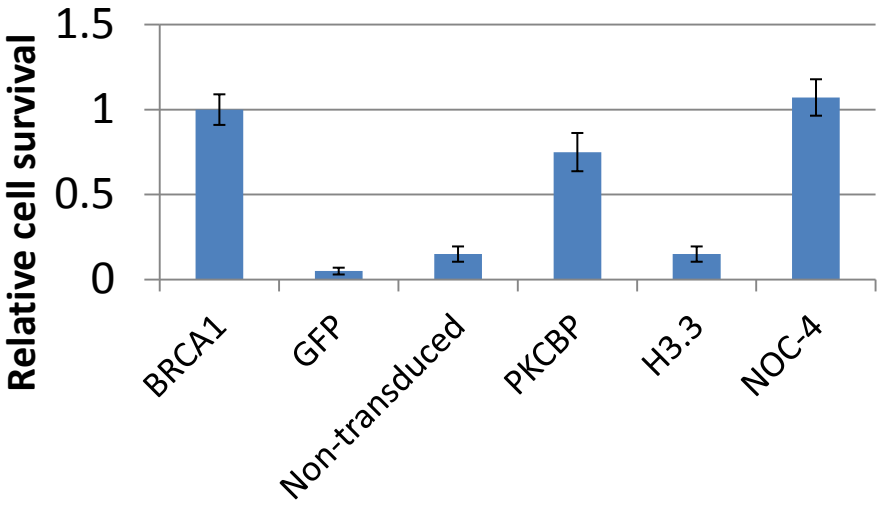

C

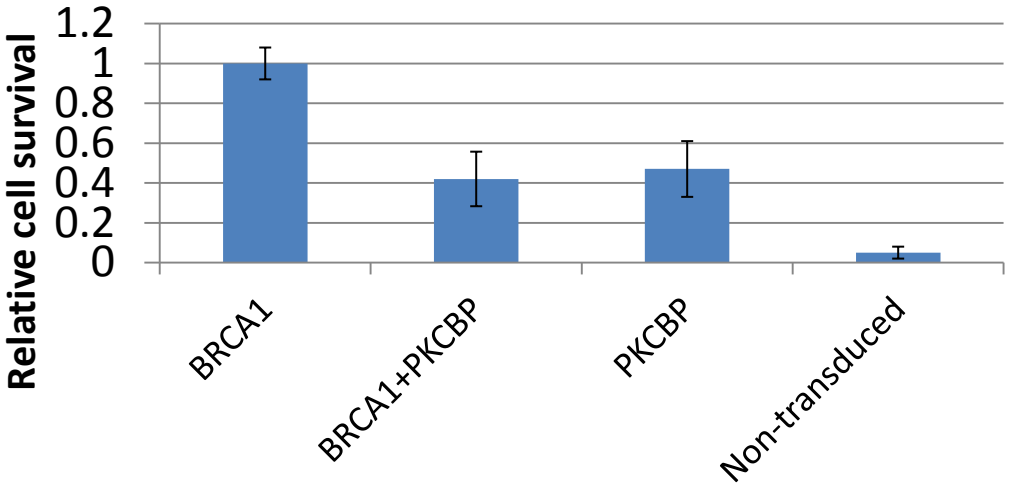

D

A

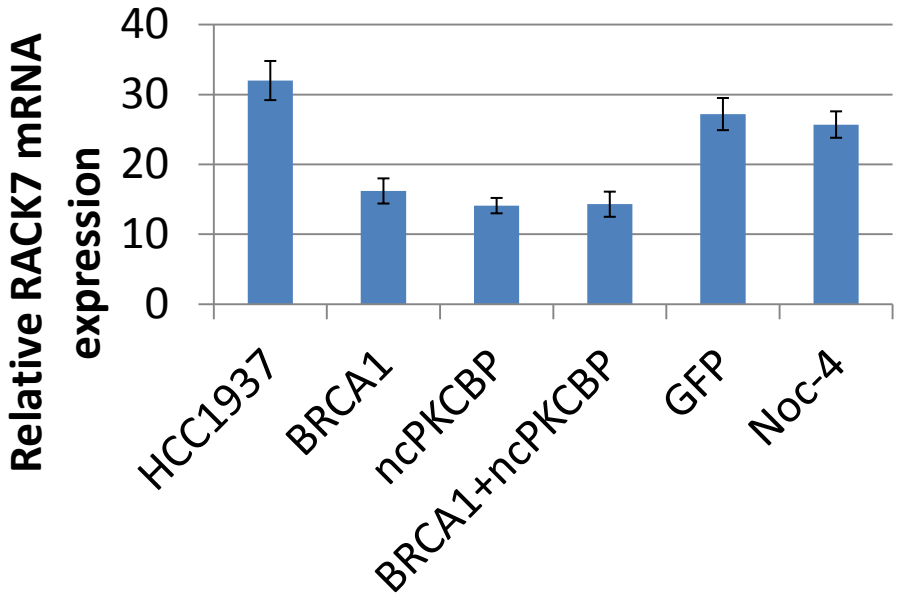
Relative RACK7 mRNA expression
40
30
20
10
0
HCC1937
BRCA1
ncPKCBP
BRCA1+ncPKCBP
GFP
Noc-4

B

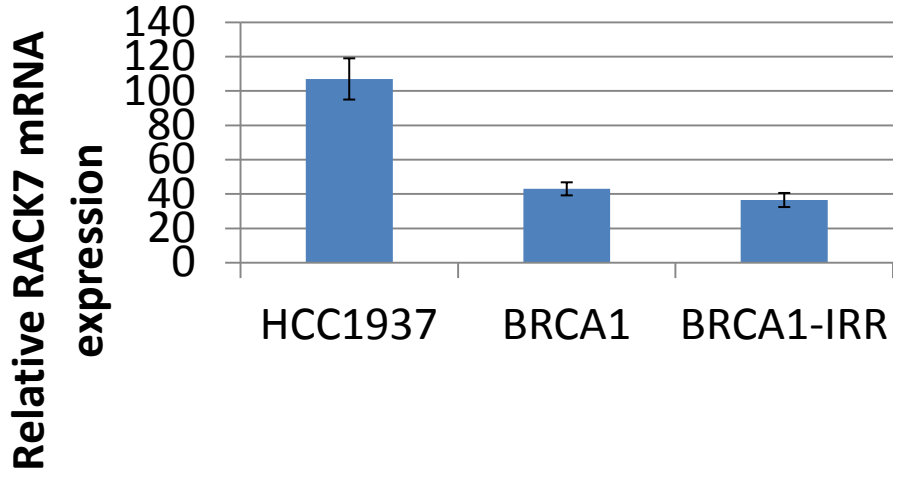
Relative RACK7 mRNA expression
140
120
100
80
60
40
20
0
HCC1937
BRCA1
BRCA1-IRR

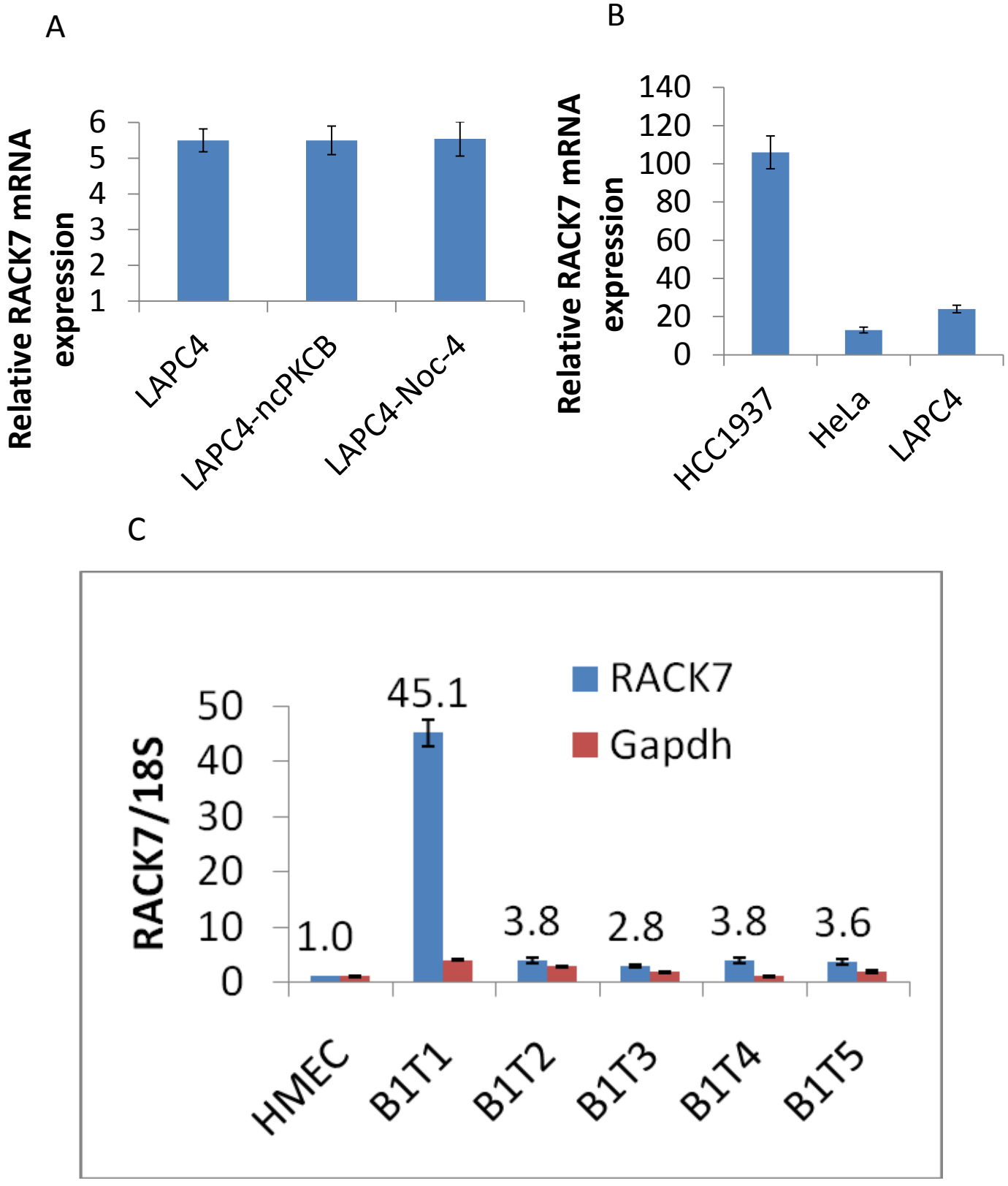
A
Relative RACK7 mRNA expression
6
5
4
3
2
1
LAPC4
LAPC4-ncPKCB
LAPC4-Noc-4
B
Relative RACK7 mRNA expression
140
120
100
80
60
40
20
0
HCC1937
HeLa
LAPC4
C
RACK7/18S
50
40
30
20
10
0
45.1
1.0
3.8
2.8
3.8
3.6
RACK7
Gapdh
HMEC
B1T1
B1T2
B1T3
B1T4
B1T5